Testing bifurcation stability for both river and tidal systems in a physical model

Master Earth surface and water, Coastal Dynamics and Fluvial Systems track

Faculty of Geosciences,Department of Physical Geography

Author:
Kaspar Sonnemans B.Sc.

Supervisors:
Prof. dr. M.G. Kleinhans
Dr. M. van der Vegt

Utrecht University

hydralab+

Abstract

River and tidal networks form important routes for the transportation of goods to and from sea ports. These networks are made up of different nodes connecting different sections, confluences and bifurcations. While a lot of research has been done on confluences, focus on bifurcations is relatively new. In tidal estuaries bifurcations occur in the form of tidal bars and rivers experience avulsions and can start to bifurcate in deltas. Bifurcation is an important mechanism in the distribution and partitioning of flow and sediment of two downstream channels and can thus influence the entire network. When this distribution leads to a dominance of one channel over the other, resulting in aggradation in one channel and erosion in the other we call this bifurcation instable. Stable behavior is described when discharge and sediment transport is divided equally. Modelling solutions have been sought after and found to better understand discharge and sediment transport division at bifurcations in rivers, and the instability or stability that it can provide. The most recent theory by Bolla Pittaluga et al. (2015) describes a relationship between the width to depth ratio and sediment mobility upstream of the bifurcation and the stability configuration of the bifurcation. There is however still a lack of both experimental and field data for intermediate and high mobility flow conditions in sandy rivers. For tidal channel systems there is no evidence that the same models and theory apply due to a lack of research. The aim of this thesis is to test bifurcation stability under changing width to depth ratios for both intermediate and high sediment mobility. During Influences of changing bank morphology and channel curvature are minimized. Experiments were also conducted to test whether the same stability theory applies to tidal channels. The experiments were done in HR Wallingford's Fast Flow Facility, a 70m by 40m flume capable of producing flow discharges in two directions. The large size of this flume made it possible for experiments on a 28 meter long sand bed, split into two symmetrical channels by use of a splitter plate of 16m long, to be conducted at intermediate and high Shields sediment mobilities. The morphological evolution of the sand bed after a perturbation was placed in one of the channels was measured by use of laser scanners. For intermediate mobility experiments with a high width to depth ratio of the upstream channel resulted in an increase of the perturbation between the two channels, indicating instability, while the bifurcations with a low width to depth ratio reduced the perturbation and were found to be stable. The same results were observed for high mobilities. It was thus concluded that, in absence of any curvature and morphology creating transverse flow differences, the width to depth ratio of the upstream channel can predict the stability or instability of the bifurcation. Additionally, experiments were conducted with symmetrical tides at intermediate Shields stresses. The experiments resulted in the same trends, with low width to depth ratios resulting in stability and high width to depth ratios of the upstream channels resulting in instability of the bifurcation.

Acknowledgement

In a discussion over dinner before band practice my drummer tried to explain me how we might be getting close to base reality. However intriguing and incredibly educating this discussion was, after finishing this thesis I can't help but feel that there is still a whole universe to be studied. It has been incredible to have been a part of this cutting edge research and meet some amazing people. I would like to use this page to properly thank a number of people.First of all, I would like to thank Maarten Kleinhans, who has been a great and understanding supervisor. It was unfortunate that it was impossible for you to attend the experiments in Wallingford, but your instructions and more importantly your trust have helped me grow from a uncertain student into a confident researcher. Thank you for being involved and understanding and giving me the time and space to address all the important things of life.
I would like to thank everybody involved in this research project, and especially the people that accompanied me in Wallingford: Michele Bolla Pittaluga, Maarten van der Vegt, Allessandro Sgarabotto, Sophia Bats, Lisanne Braat, Jasper Leuven and David Todd. Without all of you I would not have been able to have accomplished what I have done. All of you have helped me push the project and myself to the limit!
I would like to thank Hydralab+ for giving me this amazing opportunity and HR Wallingford and all their employees that were invaluable for this project.
I want to thank my loved one, friends and band for all their support and interest in my work. They provided me with both the inspiration and distraction that I needed to finish this thesis.
Finally I would like to thank my parents, for all the love they have given me and who they have seen me become.

Content

1 Introduction

The earth has a rich variety of tidal and fluvial systems which form intriguing channel patterns and networks (figure 1). These patterns are susceptible to change with every flood or tidal cycle that they go through. Current models fail to forecast these natural dynamics, yet main channels are economically important shipping fairways, whilst shoal areas that emerge and submerge daily are ecologically valuable habitats. Human interference, changing river discharge and sea level rise threaten all functions. Furthermore, there are strong indications that fairway deepening leads to reduced urban safety due to enhanced flow resistance by groynes in rivers increasing water levels and enhanced tidal range in estuaries (e.g. Bolla Pittaluga et al., 2015; Seminara et al., 2011). This enhances dike failure risk during low water level and flooding during high water level. Therefore there is an urgent need for dynamic forecasting models to optimize management strategies for these multiple functions (Wang et al., 2012; Coco et al., 2013).

Figure 1.1 Satellite images of fluvial and tidal systems displaying bifurcations and confluences (A, Jamuna. B, Mekong delta. C, Scheldt estuary)

The phenomena studied in this thesis are firstly river bifurcations and secondly the mutually evasive ebb- or flood-dominated channels that form around bars and are found in all sandy tidal systems in the world

(van Veen 1949). The cause for the mutual evasion is still incompletely understood despite the fact that they also appear in our numerical model results and experiments (Canestrelli et al., 2010; Kleinhans et al., 2015). When closely investigating the nodes where ebb and flood channels connect they can be described as asymmetric bifurcations where the ebb flow has a preference for one channel and flood for the other. As such bifurcation in these systems are critical in partitioning the flow and sediment through the channel network. Bifurcations in such systems thus have a governing role in the splitting and merging of bars and heavily influence the use of shipping lanes through the forcing of bed steps. It is still mostly unknow whether there are stability and equilibrium configurations for tidal bifurcations except for one recent theory (Wang et al., in prep.). There is a fair understanding of the tidal dynamics in such situations, but knowledge for the morphodynamics is incomplete, especially related to understanding the sediment division at the bifurcation.

While a good point to start is river bifurcations, our understanding in that field is still incomplete. Stability of river bifurcations has been studied for two decades in fieldwork, experimentation, linear stability theory and numerical modelling (e.g. Wang et al., 1995, see review in Kleinhans et al., 2013) and the recent theory (Bolla Pittaluga et al., 2015) synthesizes many of the earlier results as follows: In bedload-dominated rivers, symmetrical bifurcations are unstable and develop towards a highly asymmetrical division of discharge and sediment. The same is the case for suspended sediment-dominated rivers, but the theory predicts stable bifurcations for intermediate sediment mobility. However, there is very little data for conditions intermediate between low and high mobility rivers. Moreover, It is still unknown whether bifurcations in reversing tidal flow are unstable for similar configurations and conditions as in rivers.

Therefore, the objective of this research was to experimentally investigate bifurcation stability in a range of sediment mobilities in unidirectional flow and reversing tidal flow while keeping other parameters constant. We conducted experiments on configurations that are entirely free of topographic forcing on the flow: straight channels split into two channels over some length and depth.

1.1 Background

The review paper by Kleinhans et al. (2013) summarizes general processes and the state of the research on bifurcations in 2013. This background section functions as an additional summary providing a required framework for understanding the hydromorphological processes studied in this thesis and reviews the paper by Bolla Pittaluga et al. (2015) in depth because of its relevance to this research.

1.1.1 Bifurcation generation processes

A bifurcation is defined as the location where a channel divides into two separate channels, dividing its discharge and sediments between the two subsequent channels. While confluences (where two channels merge to flow on as a single channel) occur in all tributary systems, bifurcations are much rarer. They can be found in the following systems: alluvial fans, braided rivers, lowland rivers with meandering or anastomosing patterns and deltas. The initiation development of bifurcations can start both erosional or depositional, but further development always involves both.
The spatial and temporal scales of this initiation differ for the different mentioned systems. As such small-scale bifurcations can be initiated by mid-channel deposition in braided river systems (Leopold and

Wolman, 1957) and in delta systems with the deposition of delta mouth bars (Wright, 1977). Larger scale bifurcations can initiate through headward incision (as occurring in chute cutoffs) or bank erosion leading to the capture of an adjacent channel or other depression (as occurring in meander neck cutoffs and braid avulsions). Erosion in lowland rivers can cause the enlargement of a crevasse during overbank flooding, resulting in full avulsion and thus a bifurcation. Each mode of initiation naturally occurs in more than one of the four settings.

The immediate trigger for the formation of a bifurcation is often a flood, as the high water levels and the high rates of the bed material transport are required mechanisms for the required deposition and erosion, but there is often an underlying reason for why the chance of bifurcation becomes higher with successive floods. Progressive channel reworking during low flows, notably in braided rivers, can also trigger bifurcation. The most recognized factor contributing to the triggering of a bifurcation is aggradation of the main channel. Promoting mid channel deposition, it can locally increase the water level, reducing the height of the bank compared to the flow level, increasing the probability of flow over bars and banks and the chance of lateral capture.

Channel aggradation occurs because of bar building, external changes upstream (such as changes in hydrological regime and/or course sediment supply) or downstream (bed level change causing hydraulic backwater effects). After the establishment of the bifurcation the two flow paths may or may not both be in sediment-transporting equilibrium. Any gradient advantages of one path over the other may increase its discharge over the other path. As such a path will capture more of the discharge if and only if its transport capacity exceeds the sediments supply to it, causing it to enlarge. The relatively steeper bed slope of chute cutoffs or crevasse splays will thus cause them to be able to grow in size. Differences in bed composition between the two paths are also relevant as it influences transport capacity and consequently might infer preference for the bed with a higher transport capacity. Major crevassing in the lower Mississippi valley occurs preferentially where the banks are made up of sandy sediments that have a higher transport capacity (Aslan et al., 2005).

Another important factor for the balance of the bifurcation is how sediment is transported, either in suspension, as bedload or as both. A fourth factor, and of major interest for this thesis, is the distribution of water discharge and bed-material flux just before the bifurcation. The next section gives an in-depth overview of the known processes that govern the division of flow between the different paths.

1.1.2 Flow distribution and bifurcation evolution

It is important to understand the processes occurring at bifurcation locations to understand why and how they evolve over time. The main factor governing the evolution of the bifurcation is the discharge distribution over the two channels. If we call the different measures of discharge Q_0 for the upstream channel and Q_1 and Q_2 for respectively the larger and smaller branch, the asymmetry of distribution can be calculated through $(Q_1 – Q_2)/Q_0$, which varies from 0 for $Q_1 = Q_2$ and 1 when there is no discharge at all in Q_2. The geometry of the different channels, their width, depth, slope and sediment, will influence the possible velocities and thus discharges. The rule of the path of least resistance governs, meaning that water naturally divides its discharge to experience as little bed roughness or shear stress as possible. As such a larger (deeper and wider) channel would receive more of the discharge than a smaller channel. Or, as often seen in chute cutoffs, a channel over a larger slope with more and easier erodible sediments can be preferred by the water, causing it to gain discharge dominance.

The higher resistance of smaller channels compared to a single bigger channel causes the flow to experiences a slight uplift upstream of the bifurcation. This process, called the backwater effect, has an

important effect on the flow velocity. The increase in water depth can cause the velocity to decrease below the threshold of motion and thus causing the local deposition of sediments. As such, the sediment transport in and just in front of the bifurcation influences local bed roughness. The generation of bedforms in the area upstream of the bifurcation can influence the flow in such a way that the flow concentrates into one channel over the other. Channel curvature can also produce such concentrated flow and a preference of flow based upon upstream flow conditions through secondary circulation. Secondary flows can produce strong preference in lateral sediment transport direction, causing the sediment transport to be concentrated into one channel.

The discharge division between the channels will thus be decided by the channel dynamics of the bifurcate channels and the upstream characteristics of the flow. The transport of the sediment is related to the discharge but not linearly, meaning that although discharge can be asymmetric the channels can still be in a quasi-stable state. Such relation between discharge and sediment transport is stronger for suspended sediment transport and weaker for bedload transport. Suspended sediment is transported throughout the whole water column although in higher concentrations near the bed, while bedload transport is only transported in the lowest part of the water column. As such, bed roughness can cause sedimentation of a big part of the suspended sediment load through perturbations and interactions with the bed. As stated by Slingerland and Smith (1998) a branch with a small abruptly higher bed may receive a smaller proportion of the sediment flux than of the discharge.

An asymmetry between the discharge and or sediment transport between the two channels can be generated through any sort of perturbation in one of the two channel geometries (figure 1.2). This causes a morphological feedback loop. The perturbation reduces or increases the flow in the perturbed channel causing a decrease or increase in sediment transport. This change in sediment transport will in turn either cause for increased erosion in case of increased flow or deposition in the case of decreased flow. Through the interaction between the two channels an opposite reaction will take place in the unperturbed channel. As such, if there is deposition in the perturbed channel the unperturbed channel will have increased erosion as it takes on more of the discharge and gain a higher capacity for sediment transport.

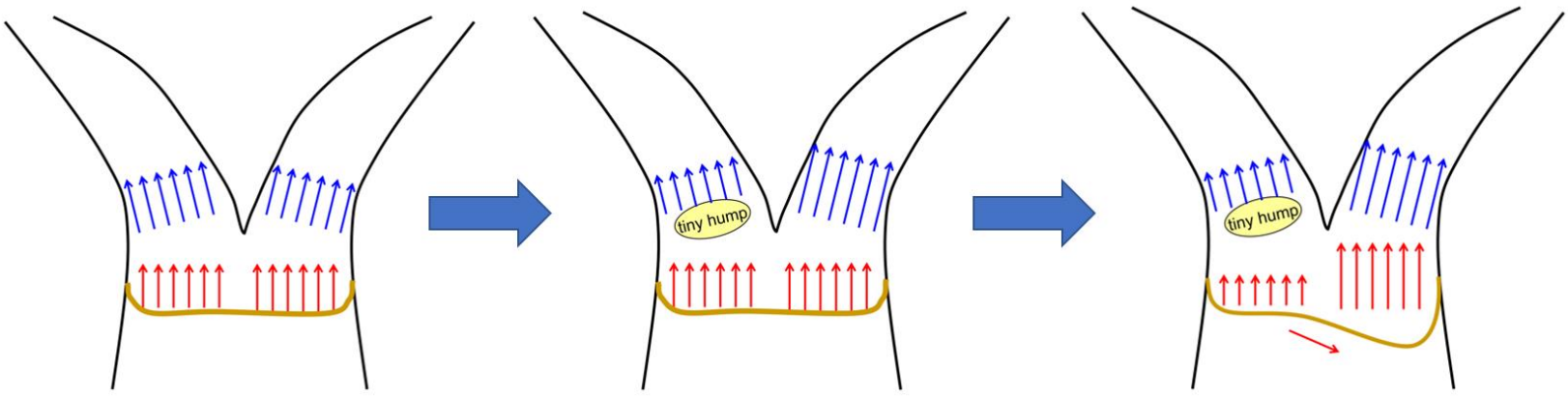

Figure 1.2 Schematic drawing of perturbation of a symmetric bifurcation. Blue arrows here symbolize discharge and red arrows sediment transport. The perturbation, in this case a small hump of sediment in the opening of one of the channels, will reduce the discharge in this channel and divert it into the other channel. This will cause erosion of the unperturbed channel and aggradation of the perturbed channel leading to instability of the bifurcation. If a strong enough transverse slope effect sediment flux is generated, the sediment input into the unperturbed channel will counter act its higher transport capacity and can lead to stability of the bifurcation.

The morphology can influence the flow in this loop through the backwater effect but also through the traverse bed slope effect. This traverse bed slope effect, caused by a lateral slope created upstream of the bifurcation through a difference in bed level, can produce a lateral transport of sediment into the deeper channel (Baar et al., 2017). Factors such as the traverse bed slope can thus have a stabilizing effect on the rate of change of the channel dynamics and even lead to quasi stability. Similarly, the effects of migrating bars into one of the bifurcate channels has a destabilizing effect on the bifurcation (Schuurman & Kleinhans, 2015). Such bar migration should however be considered an external perturbation and not an internal reaction of the bifurcation system.

1.1.3 Modelling bifurcating channels and their stability

The possibility of the stable and quasi stable bifurcation is something that has been studied for a long time. This research forms a major backbone for this thesis and should thus be studied in depth to understand the current developments within this field. The first theoretical analysis on bifurcations stability, ultimately ending in the abandonment of one of the channels, was performed by Wang et al. (1995). They studied the Rhine delta where channels are composed of mainly sandy beds with some gravel in a 1D model and proposed a 'nodal point relation'. A nodal point is required because of this 1D nature of the model. The relation states that the bed material load Q_b entering from the upstream channel is divided in the downstream branches according to the relation:

$$\frac{Q_{b_1}}{Q_{b_2}} = \left(\frac{Q_1}{Q_2}\right)^{k} \left(\frac{w_1}{w_2}\right)^{1-k} \quad (1)$$

k in this relation is some relative constant. The relation assumes that the sediment supply per unit width follows $qb \neq q^k$ where q=Q/w is the unit of discharge. Wang et al. (1995) then showed that a symmetric bifurcation can only keep on existing if $k > n/3$, if the sediment transport capacity does vary as a *n*th power of the water velocity v. Values of *k* that were lower than *n*/3 always resulted in abandonment of one of the two channels.

This research still had several limitations though. The critical value of *k* was hard to constrain and estimates of *k* from different measurements vary greatly. Another limitation is that the symmetry of equation (1) is based upon the assumption of a uniform transverse distribution of water and sediment flux in the channel upstream of the bifurcation. Upstream channels that are curved (so that q varies laterally although the depth is uniform) and/or have asymmetric cross sections however do not have such uniform flow. Making the relationship only applicable for uniform flow.

The theoretical analysis done by Bolla Pittaluga et al. (2003), designed mainly for braided gravel-bed rivers, allowed for the transverse flows of water and sediment due to an 'inlet step' difference in bed elevation between left-hand and right-hand bifurcates. The rationale behind this inlet step is that the two branches share the same water level but might have different bed elevations caused by aggradation or erosion (or a perturbation). The BRT, which is how we will reference the model, uses a logarithmic flow resistance law, threshold-excess bedload law, Exner type sediment continuity equations along both sides of the bifurcation and a quasi-2D treatment of the channel upstream for a few channel widths. The difference in bed elevation between left and right is assumed to develop progressively over a few channel widths upstream from the point of bifurcation while transverse components of water and sediment flux in the transition zone are modelled in 1D fashion, as done in the 1D model by Ikeda et al.

(1981). These transverse fluxes turned out to be critical for the evolution of bifurcation in the BRT model. Possible equilibrium states found were dependant on the aspect ratio of width to depth and the non-dimensional shear stress θ (Shields number) in the upstream channel. θ is defined as:

$$\boldsymbol{\theta = \frac{\tau_0}{(\rho_s - \rho) g D_{50}}} \ (2)$$

where τ0 is the fluid shear stress (N/m2), ρs is the sediment density (kg/m3), ρ the water density (m/s2), and D50 is the median bed grain size (m). For θ values that are greater than around 0.01 *width to depth ratio* the model predicts a stable equilibrium with both bifurcating branches staying open. Such parameters are feasible for sand-bed rivers but unlikely for gravel-bed rivers. When the slope of the two branches is equal they will also have the same discharge and sediment load, which is likely in braided rivers where branches rejoin each other after a short distance. When the slope of one branch is significantly higher it will take on more of the flow and sediment load, while sustaining a lower bed elevation.

This reactional behavior to the change in width to depth at a given Shields stress is described by equation 3 (Bolla Pittaluga et al. 2003):

$$\boldsymbol{\left(\frac{3}{2} + \frac{2.5}{C_a}\right) + \frac{8\alpha r}{\beta_a \sqrt{\theta_a}} = m \frac{\theta_a}{\theta_a - \theta_{cr}} + \frac{1}{n} \frac{dn}{dD}\Big|_{\varepsilon} D_a} \ (3)$$

This equation shows the relation for the threshold conditions for stability of symmetrical bifurcation. The equation is a function of the Shields number and aspect ratio of the upstream channel, the dimensionless Chezy coefficient, sediment transport law exponent and coefficient m and n, the coefficient r accounting for transverse bed slope on sediment transport and α which is a coefficient that accounts for how far upstream the morphological effects decay. From this equation you can denote that the left-hand side (l.h.s) is proportional to the effect of the transverse sediment flux generated by lateral bed slopes and transverse components of flow velocity and how that influences sediment transport towards the two bifurcate channels. Larger lateral bed slopes as such will have a stabilizing effect by increasing sediment influx towards the channel now receiving more discharge. The right-hand side of the equation (r.h.s.) is proportional to the transport capacity of the two bifurcate channels as a derivative of the Shields number. The ratio between the two sides of the equation will govern the evolution of the bifurcation. When both sides of the equation are equal a stability between transverse sediment transport and the transport capacity between the two channels is reached, resulting in no further change through erosion and sedimentation without a new perturbation. When the l.h.s. is larger the sediment flux over the transverse serves to transport more sediment towards the channel with an increased transport capacity. It then receives more sediment than that it can transport, thus stabilizing the bifurcation and reducing the amount that the system was perturbed. If the r.h.s. is larger it means that the increase in relative transport capacity in one of the channels is larger than the extra amount of sediment supplied to this channel thus causing it to increase the instability of the system by increasing the initial perturbation. As a higher w/d ratio of the upstream causes the effect of the l.h.s. of the equation to decrease it can be understood that our intermediate Shields stress results, while having a similar r.h.s. value, would have an unbalanced amount of sediment transport leading to an increase of the perturbation over time. Bolla pittaluga produced stability diagrams (figure 1.3) based on Shields stress and width to depth ratio values.

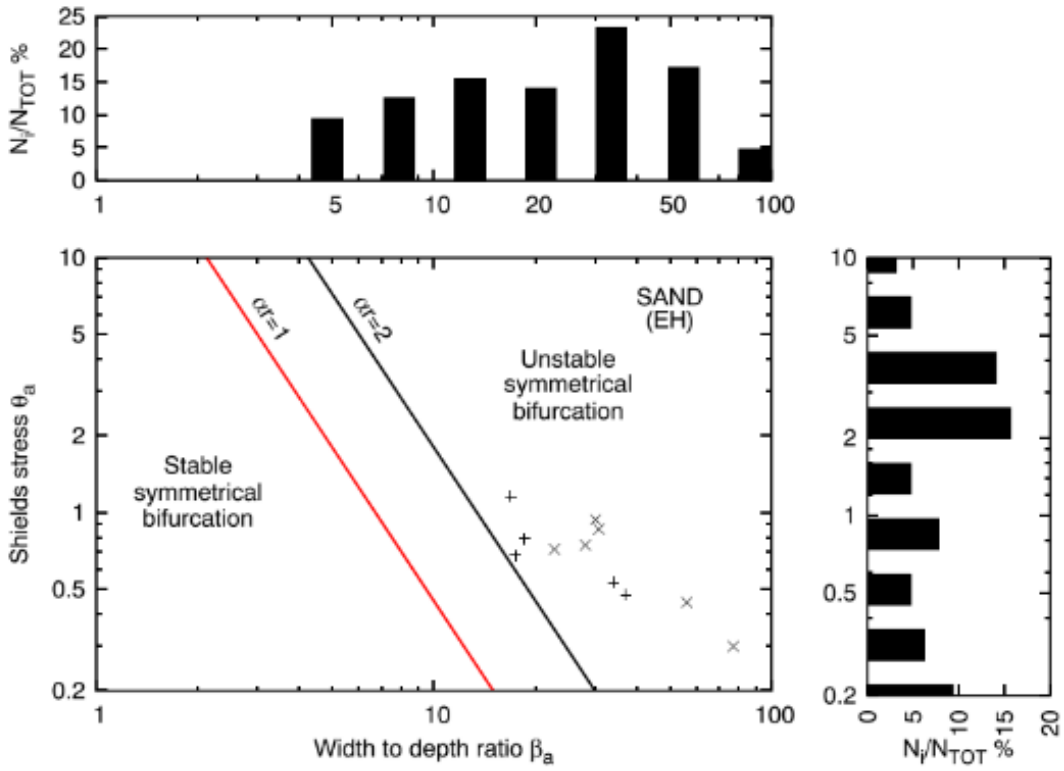

Figure 1.3 Stability diagram for sand bed rivers between upstream channel width to depth ratio and Shields stress from Bolla Pittaluga et al. (2015). Graphs above and next to the diagram show occurs rate.

The BRT model has been extended upon in several subsequent papers. Miori et al. (2006a) included an irreversible increase in branch width as discharge increases, based on the assumption that bank erosion and scour processes in braided gravel-bed rivers occur equally fast, while aggradation occurs without narrowing. This extra degree of freedom resulted in stable equilibria with a very unequal distribution of discharge and sediment load in the different branches. The effects of migrating bars in the upstream channels, leading to discharge fluctuations in the discharge ratio of the downstream branches were researched by Miori et al. (2006b) and Bertoldi et al. (2009a, b). Furthermore, the effects of curvature of the upstream channel were introduced by Kleinhans et al. (2008). The modification included changes in the equations for transverse fluxes to allow for curvature-induced secondary circulation. These modifications to some extent offset the effect of the traverse bed slope. A consequence of curvature induced flow that has a significant effect but is not yet incorporated in the model is the lateral sorting of bed material. A later extension on the model by Kleinhans et al. (2012) further combined the curvature effect with channel width dependence on discharge. The loss and input of sediment from deposition and erosion of banks were incorporated in this model. This resulted in longer avulsion times as channel depth decreased more slowly if the width also decreased in the closing branch so that water depth and sediment transport capacity remained higher.

The BRT model has been tested using both experimental and field data, which has yielded good qualitative consistency and a reasonable quantitative agreement. The field data measured by Zolezzi et al. (2016) in seven braid bifurcations showed that inlet steps and traverse bed slopes of the approximate

size were present. They found that the discharge was distributed more asymmetrically at low flow than high flow conditions. Experiments done on a Y-shaped mobile bed bifurcation with fixed banks, executed by Bertoldi & Tubino (2007), showed that the predictions of the model corresponded with the measured values. But also showed the fluctuation in discharge over time in the two channels caused by the migration of alternate bars. The nodal relation was also tested against 3D simulations by Kleinhans et al. (2008) and Kleinhans et al. (2011). They found that the initial nodal relation overestimates the traverse sediment flux. Modifications in the models to include curvature sediment balance of bed and banks however, led to models that predicted the duration of avulsions at the apex of the Rhine delta more realistically.

1.1.4 Effects of planimetric bifurcation shape on bifurcation stability

All the theoretical models as discussed so far were based on uniform flow conditions. The flow around a bifurcation is however far from uniform and should be considered much more as highly three-dimensional. Secondary flows for instance induced through curvature can make the flow into branch channels similar to flow in sharp meander bends (Neary and Odgaard, 1993). Such flow conditions can lead to the accumulation of sediments which in turn can reduce flow conveyance.
This was further illustrated by the experiments by Garde and Ranga Raju (1978) which showed that sedimentation was higher for bifurcation angles of 30-45 degrees and the least around 120 degrees. This shows that the larger secondary flow conditions caused by the angle at which the flow enters increases the sedimentation.
Naturally such larger bifurcation angles occur in rivers where banks are resistant to the relative strength of the flow, as is the case in meandering rivers flowing through vegetated and cohesive banks. Along with secondary flow such cohesive banks can also cause deep scour holes, vortex bars and horizontal flow separation that may further affect the division of flow and sediment into the different bifurcation branches. It is still hard to fully understand the critical bifurcation angle that causes separation of flow to occur. A direct proportionality between the change in direction and the flow curvature could explain the lack of separation for bifurcations. Here the greater bifurcation angles just concur with higher curvature and a smaller R/*w* ratio. This means that the stronger helical flow and greater transverse bed slopes are generated that cause the lack of flow separation.
3D flow structures can be calculated in numerical modelling using CFD (computational fluid dynamics) codes. Although they possibly produce a more realistic simulation of actual bifurcation dynamics it should be considered that they should ideally be checked and validated through the use of laboratory and field measurements. The uncertainty if there is a sensitivity to the choice of turbulence closure for simulated flow structures should also be considered.
Hardy et al. (2012) presented a parametric study on flow structure and partitioning in bifurcation systems. In their research they considered the dependence on bifurcation angle, angle asymmetry, asymmetry in the branch slopes and upstream curvature. The configuration that they used was simple with two channels half the width of the upstream channel that would run parallel a short distance after the bifurcation. From their results they concluded that secondary flow, similar to flow generated in a meander bend was generated just upstream of the bifurcation (at a distance of about 0.25 to 0.75 times the upstream channel width from the bifurcation), causing helicity in bifurcating branches immediately downstream of the bifurcation. They also found that the proportion of discharge going through each was highly sensitive to upstream curvature and only moderately sensitive to slope asymmetry between the

branches.
Miori et al. (2012), using a similar methodology, found that bed forms prevented the same hydraulic conditions to occur in bifurcations. The bedforms prevent the formation of depth scale secondary circulation cells. As such they found that the effects of the bifurcation were only felt for a short distance upstream from the bifurcation, despite super-elevation significantly increasing the water surface in front of the bifurcation. 3D model morphodynamic results closely resemble those of 1D models that included transverse bed slope and spiral flow effects on the bed load transport but are still much more simplified than CFD models in terms of topographical detail.
The shortcomings of the 1D and 3D solutions are that large bifurcation angles and bedforms are either neglected or parameterised. The current models for bend flow are sensitive to how the transverse bed slope effect is formulated and calculated and to the presence of bedforms and sorting of bed material.

1.1.5 Tidal bifurcation

While in river systems water obviously flows in one direction only, this research also aims to produce new insights in systems that have a change in flow direction, as occurs in deltaic systems with tides. In this case bifurcations become confluences and confluences become bifurcations through the turning of the tide. While this is certainly the case in estuarine systems with tidal bars and deltas with several distributaries, and a lot of research is being conducted into the dynamics of these bars (Leuven et al., 2016; Leuven et al., 2017; Leuven et al., 2018) little is known about the actual dynamics of the bifurcations and confluences within tidal systems. Tidal channels are often either dominant during flood flows or ebb flows giving them different flow characteristics. Flood channels are often deeper around the bifurcation of the two channels but gradually become shallower and end in a sill. Ebb channels often have a meandering character but present the same shallowing behaviour and possible ending in a sill. Due to the momentum of the tidal flow causing a time lag, the ebb flow can continue to flow for 20 up to 30 minutes after low water. Because flood flow then already starts to enter the estuary the ebb and flood channels tend to avoid each other (Robinson, 1960). Bifurcations and confluences, which effectively are both present in a tidal system, are formed around tidal bars. The papers by Leuven have analysed the dynamics and found several interesting characteristics. As such they found that bars in estuaries are similar to those in braided rivers but 30% more elongated, this means that they are on average 6.9 times as long as their partitioned width (Leuven et al., 2016). Tidal bars further resemble river bars in most aspects but do show some unique features such as the mutually evasive ebb and flood tidal channels. The influence of tidal flow has been studied for the Berau delta (Buschman et al., 2010). They found that tides enhance the subtidal flow division of deeper and shorter channels. Tidal motion was found to direct flow from the channel with lowest bed roughness to the channel with highest bed roughness.

1.2 Research questions and hypothesis

Due to the range of different parameters that are shown to influence bifurcation stability, such as bend flow, channel bed resistance and transverse bed slope effects, it is important to study each effect in isolation. Furthermore, good data to understand whether and how these parameters influence bifurcation stability in tidal channels is still unavailable. This study aims to isolate the effect of the transverse bed slope effect and challenge the BRT model. To this end, a setup was used that avoids flow curvature and bed resistance gradients in the bifurcation. Additionally, we aim to test the effects of tidal

flows on the same configuration as used for unidirectional flows. This thesis will attempt to answer the following questions:

- What are the roles of the width to depth ratio and the sediment mobility of the upstream channel on bifurcation stability?
- What are the differences between unidirectional and tidal flow conditions for bifurcation stability for different width to depth ratios and the sediment mobilities?

It is hypothesized that low width to depth ratios will increase the effect of the transverse bed slope sediment flux. The increase of sediment input into the channel with an increased sediment transport capacity should then lead to bifurcation stability and reduction of the perturbation. High transport capacity of the upstream channel however will cause the bifurcation to become unstable. Through measurement of the upstream width to depth ratio and sediment mobility it is expected that the stability of the bifurcation under these conditions can be predicted. Prior to these experiments no data have ever been collected on bifurcation stability for tidal flow conditions. The hypothesis is that stability can also be predicated by measuring the upstream conditions in the setup where upstream and downstream conditions are equal. A difference that is expected is that the rate at which tidal flow conditions will evolve into stability and or instability will be faster or slower than under unidirectional conditions due to either slowing down or speeding up of the morphological change in the bifurcate channels.

2 Methods

The objective as stated in the introduction was to experimentally investigate bifurcation stability in a range of sediment mobilities and for a number of width to depth ratios of the upstream channel in both unidirectional and reversing tidal flow. To this end physical model experiments were conducted in the fast flow facility at HR Wallingford. A nodal point model based on the studies by Bolla Pittaluga et al. (2003 & 2013) was run to test possible conditions for the experiments and to compare the experimental outcomes with the theory.

2.1 Methodology

Important aspects of the BRT model are the transverse bed slope sediment flux and transport capacity of the upstream channel. In an experimental setup these can be controlled by changing the width to depth ratio and the total flume discharge. To limit the effect of transverse flows and sediment transport other than the transverse bed slope effect the experiment was designed symmetrical and without curvature. The two bifurcate channels were of equal length and width and completely in line with the upstream and downstream channels to ensure no curvature effects in the flow. A splitter plate simulates the bifurcation and eliminates any effects on the morphological chances of the banks of the channels. To test different effects of the transverse bed slope effect experiments would be executed at different water depths to change the width to depth ratio of the upstream channel, which is an important input for the transverse sediment flux in the BRT model. Through the use of the same sediment throughout all the experiments the transport capacity or sediment mobility could be controlled through adjustment of the discharge. To answer the research questions as stated in the introductionm the experiments were setup so that their morphological evolution should clearly fall into stability or instability, as observed in figure 1.3. For as far as the available time allowed for it duplications of the experiments were conducted. This was however not possible for each configuration

2.2 Experimental setup

2.2.1 General description

The Fast Flow Facility (http://www.hrwallingford.com/facilities/fast-flow-facility) is a unique flume, setup as a racetrack with a return flow channel next to the experimental channel. The flume has a main working channel size of 70.00 m by 4.00 m, with water depths in the range of 0.85 m to 2.00 m. Set up as a racetrack, a back channel with a width of 2.60 m circulates the water. The turns in the flume are divided into bends with a smaller width so that uniform flow is produced within the main channel. A metal and foam beach construction was installed to increase the uniformity of the flow and reduce the effect of wave generation in the flume. The facility is equipped with two pumps in the back channel with a combined power capable of discharges of up to 4s.9 m^3/s, that can be directed in both directions in the flume. As the pumps can only be operated at flume water depths above 80 cm, and the designed experiments required water depths of as low as 14 cm a concrete structure was created. As such the experimental top of the sand bed was elevated 85 cm above the flume floor and created to be 30 cm deep. Two concrete ramps on both side of the sand bed will gradually decrease the water depth to the required values. Figure 2.1 shows a schematic drawing of the experimental setup while figure 2.2 shows the original schematic of the entire flume and concrete construction for the bed.

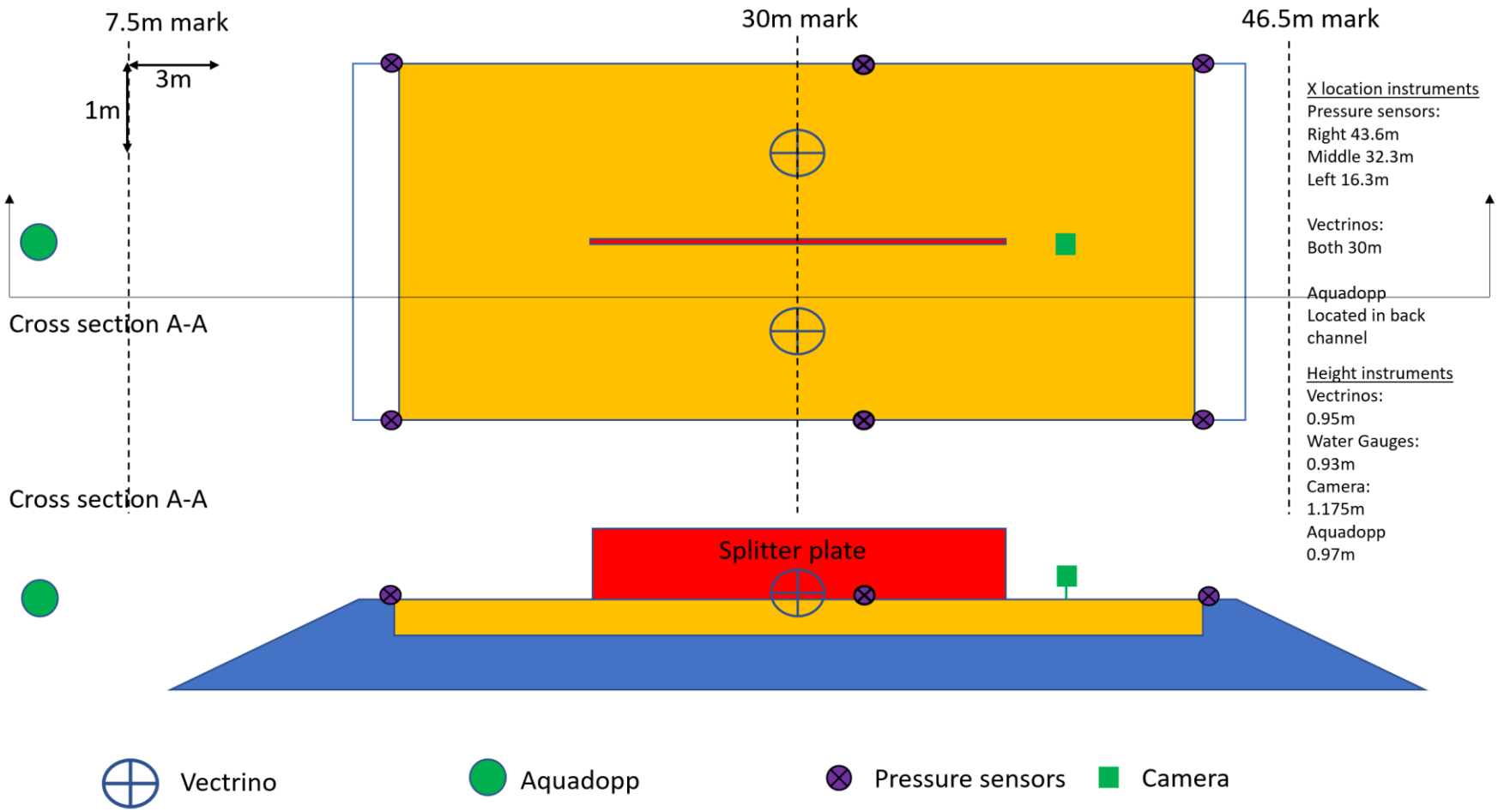

Figure 2.1 Drawing of experimental setup with the top view above and a sight view below (sec A-A). Heights of instruments measured from flume floor.

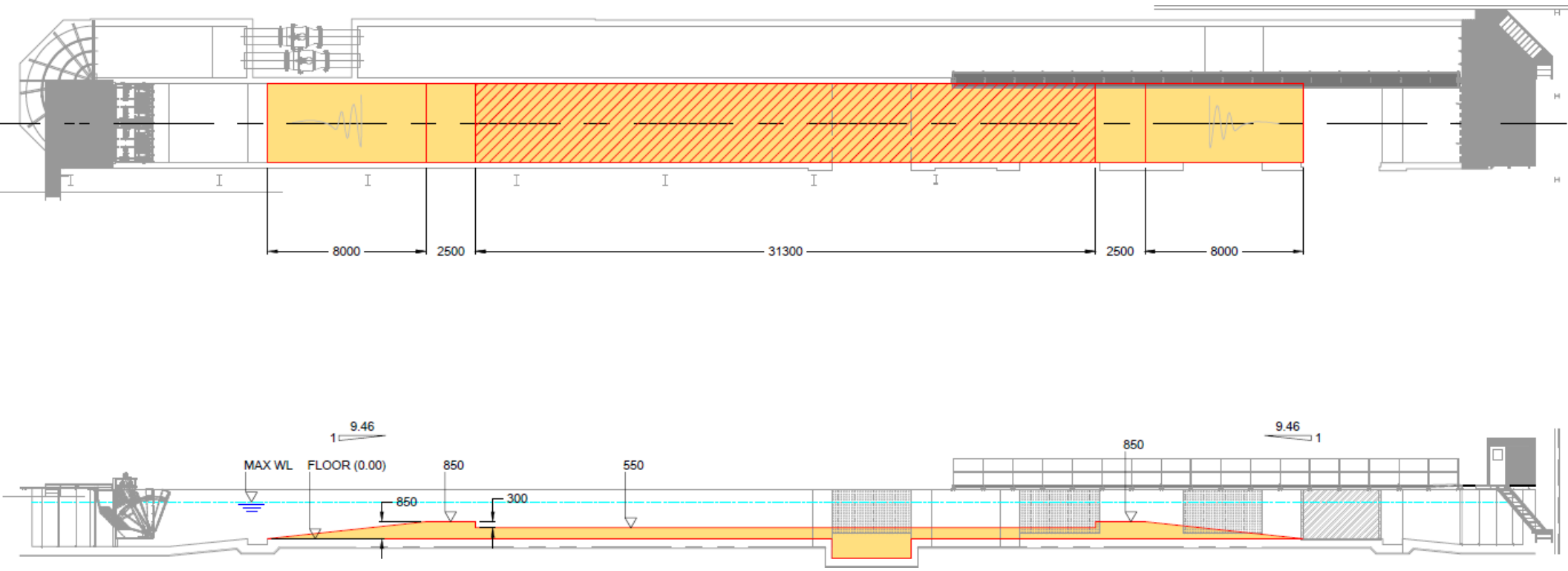

Figure 2.2 Technical drawing of the Fast Flow Facility, indicating the concrete mock bed in top view above and side view below.

2.2.2 Definition of the coordinate system

This thesis works with a coordinate system for the flume to discuss the location of measurement equipment and morphological features. The units for the coordinates are in millimeters. The origin of the coordinate system is at the opposite side of the control room, located at the far right in fig. 2.1 (x=0), at the window-side (y=0) and the floor of the flume (not the mock floor) (z=0). The left-hand, seen from the control room and with windows in the walls, side is defined as that with the lowest y-coordinates and the opposing wall is the maximal limit (y=4000). The pump operates with positive values for flow from low to higher x coordinates, and negative for high to lower coordinates. To provide the best visibility and cable routing from the control room, unidirectional flow was directed from high x coordinates to the lower x coordinates and the pumps thus run at negative pump speed values.

2.2.3 Relevant fixed parameters

The sand bed remained constant in width and length during the experiments with a fixed flat concrete part at the initial screeded bed level of Z=850 before the sand bed on each side (see Figure 2.1). The length and the position of the splitter were also constant at x=22000 mm to x=38000 mm and y=2000 mm with a width of 20 mm. For sake of consistency, upstream of the bifurcation will refer to measurements taken at x>380000 mm and downstream will refer to measurements taken at x<22000 mm regardless of unidirectional or tidal flows. The particle size distribution of the sediment was given by the supplier and reported in table 2.1. The same sediment was used for all the test particle size distribution of the sand with an average grainsize of 0.204 mm. The Flume sidewalls and splitter plate acted as unerodable banks throughout the experiments.

Table 2.1 Particle size data of the sediment.

MICRONS	BCS319 (Sieved)	
	% RETAINED	% PASSING
500	0	100.01
355	0.42	99.59
250	13.35	86.24
180	59.49	26.75
125	25.01	1.74
90	1.63	0.11
63	0.09	0.02
0	0.02	-

2.3 Instrumentation and data acquisition

2.3.1 Instruments

To analyze the stability of the bifurcation in the experiments the following instruments were used to measure parameters:

- 2 underwater line laser scanning systems for bed elevations in both parallel channels connected to a single rail on a traverser system allow for relocation over the flume X and Y directions.
- 2 vectrinos for velocity measurements in both parallel channels, both upward looking
- 6 pressure sensors for water levels along the flume, 3 on both sides of the flume.
- 1 Aquadopp acoustic device for discharge
- Imaging: underwater camera for timelapse, timelapse camera recording lab activities, hand-held photocameras and GoPro

The vectrinos acoustically measured 3D water velocity within a small beam. For the experiments only the flow in the x directions of the flume was considered. The Aquadopp measured a profile of 3D velocity through acoustic doppler effects. Through a matlab script provided by HR Wallingford the depth to the bed could be computed. Through another provided script the depth averaged velocity could be calculated to approximate discharges from the width and depth of the back channel.

The exact position and elevation of the instruments can be found in table 2.2. The underwater laser scanners were placed at a height of 630 mm above the bed to maximize scanning efficiency. The time for scanning in this setting was limited by the fill rate of the flume (approximately 1 cm per minute), and the required number of tracks to be scanned limited by the speed of the traverser system. The chosen

height optimized for these two factors to reduce the time spent scanning the bed and increased the effective use of time in the facility resulting in a scan in three tracks over the bed. The width (the y direction) of the scanned area was limited by the offset of the laser scanner and height of the splitter plate. This meant that the outer most area (along the two flume walls) could not be scanned. On the y axis the laser scanner had a range from 4200 mm to 3570 mm. The track on which the traverser system moved limited the area to be scanned on the x direction to 20000 mm 42000 mm, meaning that not the entire bed could be scanned on x axis either.

Table 2.2: Positions of instruments. The elevation of the sand bed is 850 mm.

Instrument	x (mm)	y (mm)	z (mm)
laser scanner	variable	variable, scan width ~560	1480
vectrino LHS	30000	1000	920
vectrino RHS	30000	3000	920
pressure sensor 1	16300	0	930
2	16300	4000	930
3	32300	0	930
4	32300	4000	930
5	43600	0	930
6	43600	4000	930
Aquadopp	return flow channel (2600 wide)	1300	970
underwater camera	40000	2000	1175

2.3.2 Definition of time origin and instrument synchronization

Time is given in GMT+1. Vectrinos and pressure sensors were triggered by the flume control system at 5 or 10 minutes after the start to allow for ramp up of the flow. The pressure sensors recorded the entire runtime. The vectrinos recorded at 10hz in short bursts during unidirectional flow and continuously for a tidal cycle during tidal conditions (resulting in 5 minutes of measurements and 5 minutes without measurements). The aquadopp was started manually and recorded at 1hz in bursts during unidirectional flow and continuously for tidal conditions. The laser scanning took place during temporary still flow. The steering file for the pumps defined the normal flow and reversing flow characteristics.

2.4 Measured parameters

The bathymetry was mapped during intervals in the experiment, that were chosen depending on the rate of morphological, change using the laser scanner. The number of scans per experiment was limited to only 2 or 3 scans due to time restrains. Flow velocity was measured in both channels using vectrinos in order to quantify flow conditions and changes in time during each experiment. Ripple motion was recorded with an underwater camera. A measure for the discharge was measured by aquadopp. Water levels were measured on 7 locations, 1 in the back flume (facility standard water level measurement) and 3 on each side of the main flume, located to measure the water level before, in the middle and behind the sand bed.

2.5 Experimental procedure and experimental programme

A number of experiments were conducted to test the bifurcation stability theory in unidirectional flow in intermediate and high mobility. Low mobility was impossible because of run time limitations. Tidal flows were run for comparable conditions to test stability but were limited only to intermediate mobility.

The conditions for the different experiments were chosen such that the stability or instability would be assumed according to the theory described in the BRT as can be found in table 2.3. As the upstream width of the system was constant with 4 m, the still water height of the flume would be changed to change the width to depth ratio of the system. As such the still water height of the bed was modified from 14 cm to 80 cm. The inputted discharge needed to produce the required Shields stress for the system was calculated assuming only bed load sediment using the Engelund and Hansen transport law. The experiment duration was assessed based on estimated sediment transport rate by a predictor, and tested in a nodal model, and the required time to either remove the perturbation on the bed or develop it measurably and would be stopped when conditions would change away from what we were originally testing (as is the case for experiment 5 where a large upstream bank entered the system).

Table 2.3: Experimental input conditions

experiment	run-time (hr)	depth (m)	discharge (m3/s)	(peak) velocity (m/s)	target Shields	aspect W/h	uni-directional / tidal flow	tidal period (s)	target bifurcation
4	13	0.14	0.22	0.39	0.5	29	uni		Unstab
5	35.24	0.50	0.85	0.42	0.5	8	uni		Stable
6	18	0.50	0.85	0.42	0.5	8	tidal	216	Stable
7	18.5	0.14	0.22	0.39	0.5	29	tidal	280	Unstab
8	19.5	0.50	0.85	0.42	0.5	8	tidal	216	Stable
9	2.24	0.25	0.77	0.77	2	16	uni		Unstab
10	18.5	0.50	0.85	0.42	0.5	8	uni		Stable
11	38	0.14	0.22	0.39	0.5	29	tidal	280	Unstab
12	0.9	0.80	2.60	0.81	1.5	5	uni		Stable

In total 9 experiments were conducted that can be grouped in 3 categories: unidirectional intermediate Shields stress flows, unidirectional high Shields stress flows and tidal intermediate Shields stress flows. For each category both stable and unstable situations were attempted. Two parameters for the experiments were controlled by changing (A) the water depth of the flume to change the width to depth ratio and (B) forcing the pump at different speeds to produce the required discharge for the Shields stress of interest.

The initial bathymetry was the same in all experiments, where the bed was screeded flat to a height of z=850 mm. A perturbation of either about 25 mm or 5 mm (for stable high mobility unidirectional flow), necessary to initiate bifurcation instability, was made by a sediment hump located upstream in one of the bifurcated channels (indicated in Apendix A1) over a given length and height. In some experiments the bed had not appreciably changed and was used for the next experiment in view of time limitations, also indicated in Apendix A1.

For the unidirectional experiments the pumps were run with negative (as set by the facility) pump speeds. The advantage of flow in this direction is that the upstream bifurcation would be visible from both the control room and through the window in the flume wall. This flow direction will further be considered as normal flow throughout this thesis.
For tidal flows driving files were created that would ramp up the pump speeds to the target discharge needed in one flow direction to then ramp down again to zero and back up to the target discharge in the other direction. The period for the forcing of the pump would thus simulates a tidal signal. In for this research the stable tidal experiments were ran with a tidal period of 216 seconds and unstable experiments were ran with a tidal period of 280 seconds. In our experiments we were most interested in running as much tidal periods as possible, but limits in the driving of the pumps required longer tidal periods for the unstable periods to allow for the water to stabilize before reversing flow. The period of actual flow is still close to 216 seconds, but time between switching flow direction increased the actual time of the forcing period. Important to note is that the efficiency of the pump was not the same in the two flow directions, meaning that the same rotation speed of the pump would not result in the same discharge. Another influencing factor for the pump settings was the water depth, as this also resulted in different discharges for the same pump speed for different water depths. Tests with the pumps were executed over different water depths to create appendix A2. The discharges measured with the aquadopp for these tests were used as inputs in both the tidal and unidirectional experiments.

2.6 Data post-processing

Data processing was done for both storage of the data as part of the Hydralab+ project and for this thesis. This section discusses the different degrees of data post processing for the different datasets collected.

In the experiments where the perturbation was located on the other side of the flume the results reported in this thesis have been flipped so that perturbation is also ways on the same location (between y=0 mm and y=2000 mm) while in reality the location was altered between experiments.

2.6.1 Laser scanner

The laser scanner point cloud data were recorded in a .csv file while the location of the laser relative to the traverser system was recorded in a separate .txt file. HR Wallingford software assigned x,y data to

each cloud point according to a calibrated location of the traverser system in time. Having done that noise and low intensity data are then filtered out by using a low intensity threshold or by manual cropping. The remaining data are saved in an .csv file where the calibrated and corrected to true flume coordinates x,y,z are reported in a straight line.

The laser scanner data will be filtered and gridded to obtain usable bathymetries and quantities describing bedform height and bed level variation. To summarize the scan results averages differences in bed level heights of certain bed sections were calculated and plotted over time. Figure 2.3 shows How the scanned bed was divided into a left and right measurement for the upstream, downstream and the bifurcate channels. The average of the right and left channel was calculated and subtracted from each other. The plots in the results show absolute values of the differences between the two sides of each section.

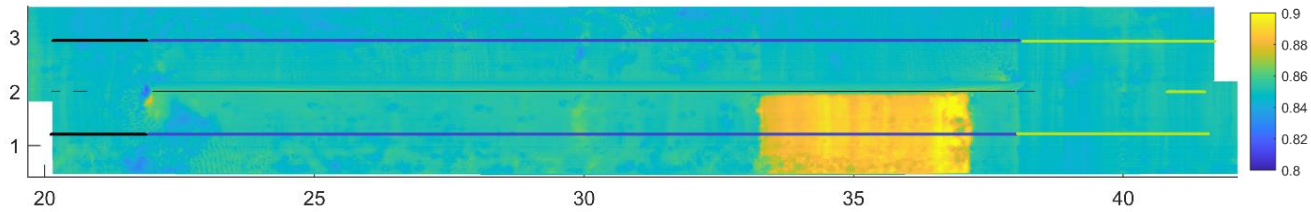

Figure 2.3 Division of bed level averages per bed section. The black lines describe downstream channels, blue lines the bifurcate channels and the green lines the upstream channels.

2.6.2 Vectrinos

The vectrino data were saved unfiltered. To calculate mean values threshold filters were used on the correlation, signal to noise and velocity of the measured data. These filters were manually found to be best at a correlation filter of 50, a signal to noise filter of 10 and a maximum of 0.2 m/s over the expected velocity. As the vectrinos measured a small profile that was most accurate in its central node, the plots given in this thesis reports unidirectional mean velocities of the central node in the profile are plotted. For the tidal experiments the median filtered smoothed maximums and minimums for both negative and positive flow directions are plotted.

2.6.3 Pressure sensors

Data is recorded as voltage which is calibrated to a known still water level. The recorded voltages are then converted to the corresponding water levels in mm using the measured height above the bed of each instrument. The only filtering done for unidirectional flow before plotting is taking out sudden drops in voltage to -10. These are recorded and converted in the data but filtered out before plotting. Because of the harmonic behavior of the water level at tidal flow a harmonic fit was ran over the water level data to provide mean water levels over time.

2.6.4 Aquadopp

The Aquadopp profiler collected time series of at least 10 minutes up to the entire length of the experiments. Using the dimensions of the back flume where it was located and Matlab scripts provided HR Wallingford discharges for all the used pump speeds at different water depths (measured above the bed) were calculated. With these discharges measurements the Shields stress on the system could be calculated.

2.7 Modelling setup.

Modelling of the experiments was executed in an adaptation of the nodal point model (takke44) used in Kleinhans et al. (2008). The model bases flow on Bélanger equation using the White–Colebrook roughness predictor. By making use of the Exner sediment conservation law and sediment transport rates based on Engelund and Hansen [1967] the morphology is updated in all points except for the nodal point. The model implements the nodal point relationship from the BRT model to iterate the discharge and sediment division at the bifurcation. For this thesis the model has been setup to model the flume dimensions and conditions. A function has been added to the model that allows for a flipping of the bathymetry on the x axis. This flipping simulates the effect that the tide has on the system in a similar way that the physical model has incorporated tides. As such the flipping occurs at a similar time frame driven by a sinusoidal vector with the same properties as the tides in the experiments. However, it should be noted that there is no relation between this tide vector and the discharge. The model results will thus run at around the peak velocity of the tidal experiments in either direction for the entire duration of the tidal cycle. This should cause a faster evolution of the morphology compared to that of the measured experimental results.

3 Results

3.1 Stable and instable bifurcations

The main research questions for this research revolves around the stability of bifurcations in both unidirectional river systems but also in two directional (ebb and flood flows) tidal systems. Table 3.1 presents the measured Shields variables and width to depth data in comparison to parameters that were intended, ordered in flow mode and Shields stress parameters. The stability of the systems was first assessed through assessing the difference in sediment transport and discharge through the two channels over time, and upstream and downstream of the bifurcation. Sediment transport is observed through inspection of the bed scans. Average heights of the two channels over time can show either growth or erosion of the bifurcate channel. The time series of the vectrinos are an indicator for showing discharge division over the two channels, though they only measure a single location thus they only form an approximation. We describe the system to be stable or converging towards a stable situation when the differences in bed levels and discharge division between the two sides of the flume decrease over time. Instability is described as an increase of the perturbation and an increase of the differences in bed level and discharge asymmetry over time. To further support the measured stability or instability of the systems the traverse bed slope upstream of the bifurcation and the hydraulic slope on each side of the flume were calculated and plotted.

Experiment	intended θ	θ Upstream	θ downstream	Intended w/d	w/d upstream	w/d downstream	Stability
4	0.5	0.65		29	25.8		No
5	0.5	0.40		8	8.0		Yes
6	0.5	0.46	0.43	8	7.6	7.3	Yes
7	0.5	0.42	0.38	29	25.6	25.5	No
8	0.5	0.46	0.43	8	7.6	7.4	Yes
9	2	2.15		16	16.3		No
10	0.5	0.40		8	8.1		Yes
11	0.5	0.44	0.42	29	25.8	25.8	No
12	1.5	1.37		5	5.1		Yes

Table 3.1: Experiment intended and measured Shields values and width to depth ratios.

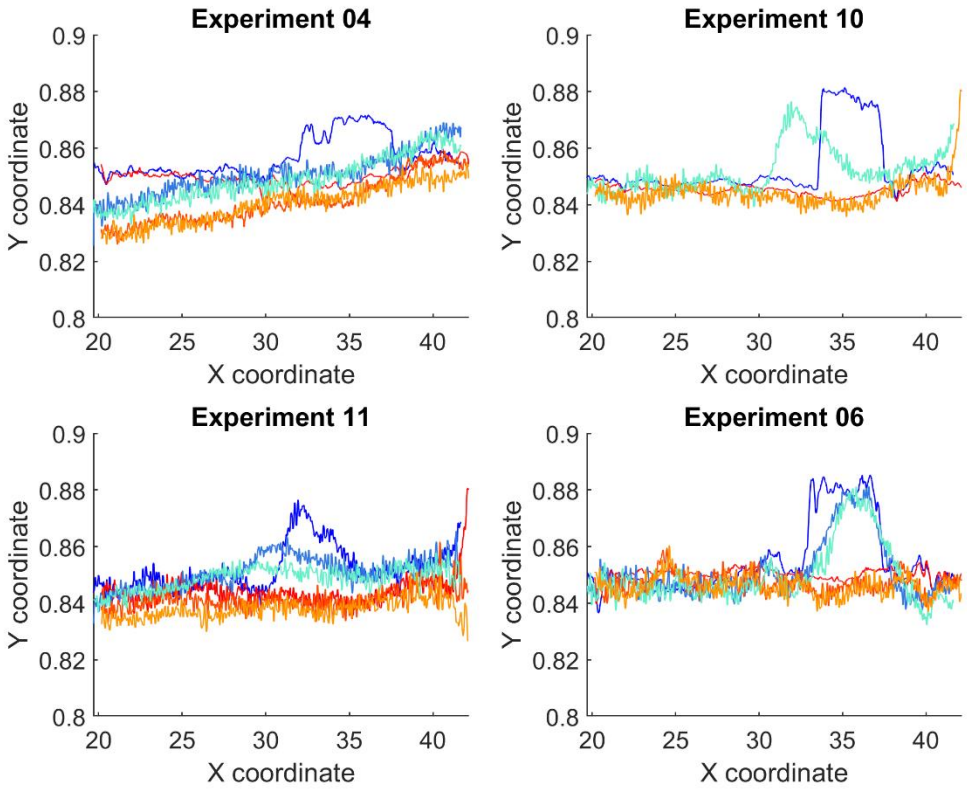

Figure 3.1 Average bedlevels for left and right sides of the flume, blue to light blue for the evolution of the perturbed bed and red to orange for the unperturbed bed. Evolution over time of the laser scanner data provides an indication of trends in erosion and sedimentation. Flow directions is from high to low x coordinates for unidirectional flow, and either direction for reversing tidal flow.

3.2 Unidirectional flow experiments

Five experiments were conducted for unidirectional flow, of which three were at intermediate Shields stress and two at high Shields stress. The duration of the high Shields stress experiments was very limited because of the high impact on the sand bed due to the high rate of erosion of this flow. The most important data collected to investigate stability of the experimental bifurcation was the laser scanner data (figure 3.1). Vectrino and pressure sensor data provided extra indicators of flow conditions.

3.2.1 Intermediate Shields stress low width to depth ratio, stable bifurcation.

Experiment 5 and 10 (low width depth ratio and intermediate mobility) in general showed a slow removal of the perturbation and reducing depth difference between the perturbed and unperturbed channel. Figure 3.2 and 3.3 show the bed evolution through digital elevation models (DEMs), the splitter plate is plotted in black. The initial scans (scan 1 for bot figure 3.2 and 3.3) shows the perturbation by the addition of a bump of sand in one of the channels. The average height of the perturbed channel decreases through erosion while the unperturbed channel fills up a bit until they reach a situation that is

close to stability for experiment 5, shown by a decrease in difference in average bed height. In experiment 10 a decrease in difference between the two channels is observed but not quite as pronounced as for experiment 5. The average bed elevation upstream and downstream of the bifurcation on both sides (figure 3.4) indicate that the system is towards a more equal distribution of sediment transport. During 17 hours of experimentation the difference between the downstream channels remains very small in both experiments. Continuing the experiment longer resulted in a difference between the two downstream channel parts of about 3 mm in experiment 5.
The measured average velocities were initially lower in the perturbed channel than in the larger channel but became more equal over time in accordance with the bed level development. For experiment 5 the velocities take about 10 hours to converge. Similar flow velocities are also observed in experiment 10 after 10 hours, but the difference in velocities in the hours before is not as pronounced for this experiment and seems to grow bigger a bit further into the experiment. Water surface slope fluctuations (figure 3.5) were caused the by passing of a large transverse bedform at the location of the pressure sensors. In experiment 10, where the experiment was stopped before being as influenced by transverse bedform as experiment 5. It is visible that the water slope for both sides of the channel was equal.
Figure 3.6 show the average transverse bed level for both the upstream, and downstream sections of the flume. While the difference between the left and right side upstream remains very stable in experiment 5, it increases slightly in experiment 10. The figure also shows how both upstream and downstream there is no to little transverse slope. Under these intermediate flow conditions, the unperturbed channel shows less erosion and possibly even some deposition (experiment 5 in figure 3.2). The perturbed channel however shows clear erosion on both the perturbation and rest of the channel.

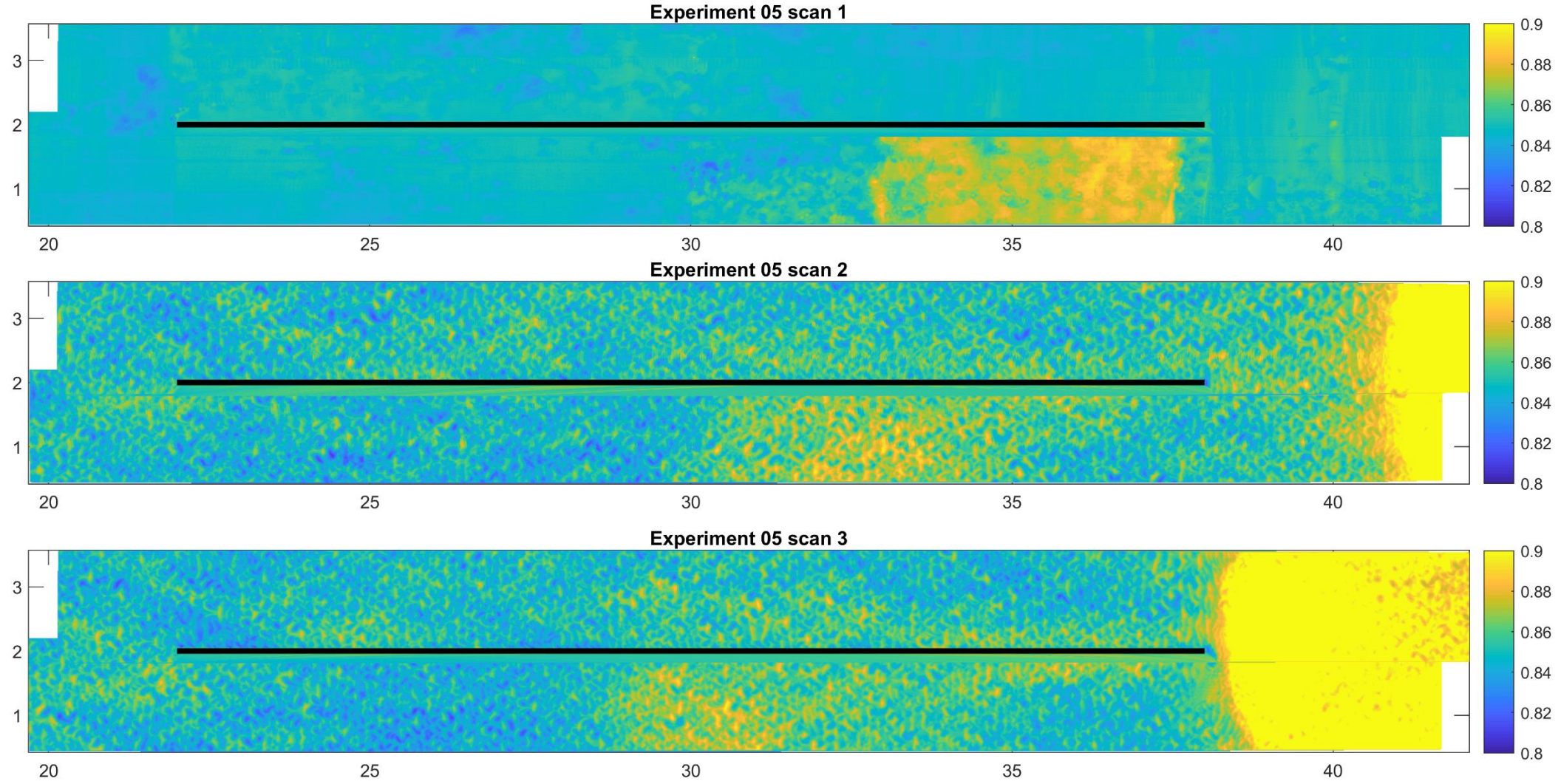

Figure 3.2 Digital elevation model for the different scans made for timeseries for intermediate Shields stress, low width to depth ratio, hypothesized stable bifurcation, in experiment 5. The black line shows the splitter plate location. X and Y axis are the flume coordinates in meters. Original perturbation is visible as higher section in the left (y <2) channel. Flow direction was from high to low x coordinates (right to left). Scan taken after: scan1 t=0h, scan 2 t=16.5h, scan 3 t=35.24h

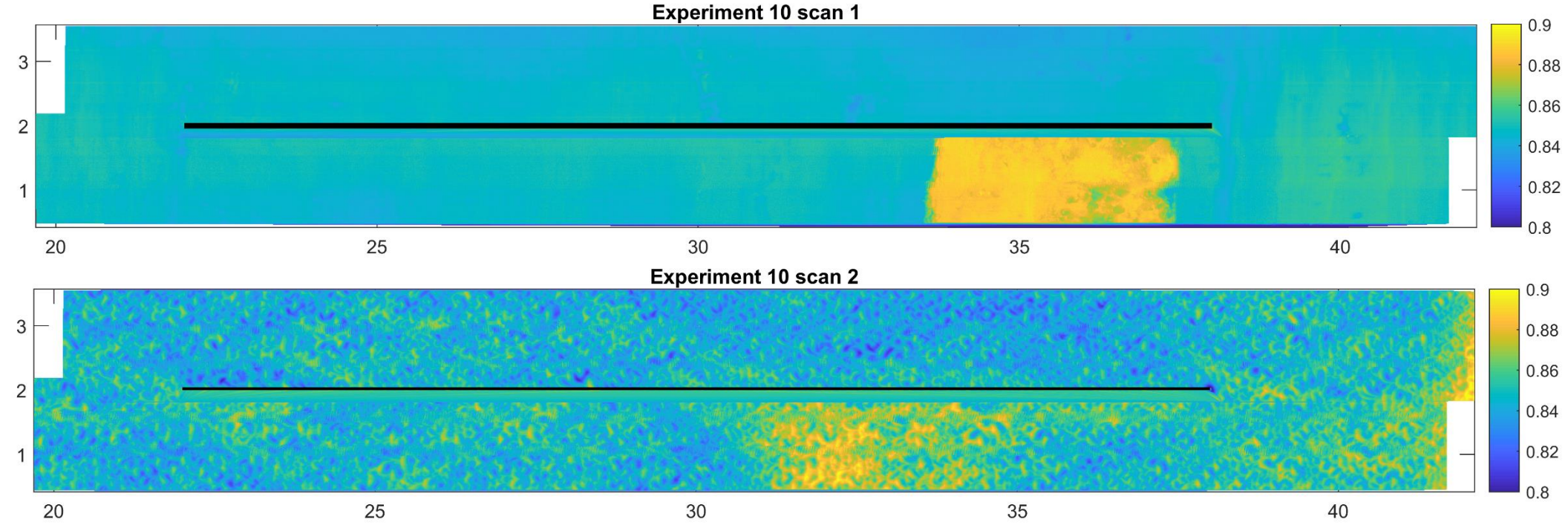

Figure 3.3 Digital elevation model for the different scans made for timeseries for intermediate Shields stress, low width to depth ratio, hypothesized stable bifurcation, in experiment 10. The black line shows the splitterplate location. X and Y axis are the flume coordinates in meters. Original perturbation is visible as higher section in the left (y <2) channel. Flow direction was from high to low x coordinates (right to left). Scan taken after: scan1 t=0h, scan 2 t=18.5h

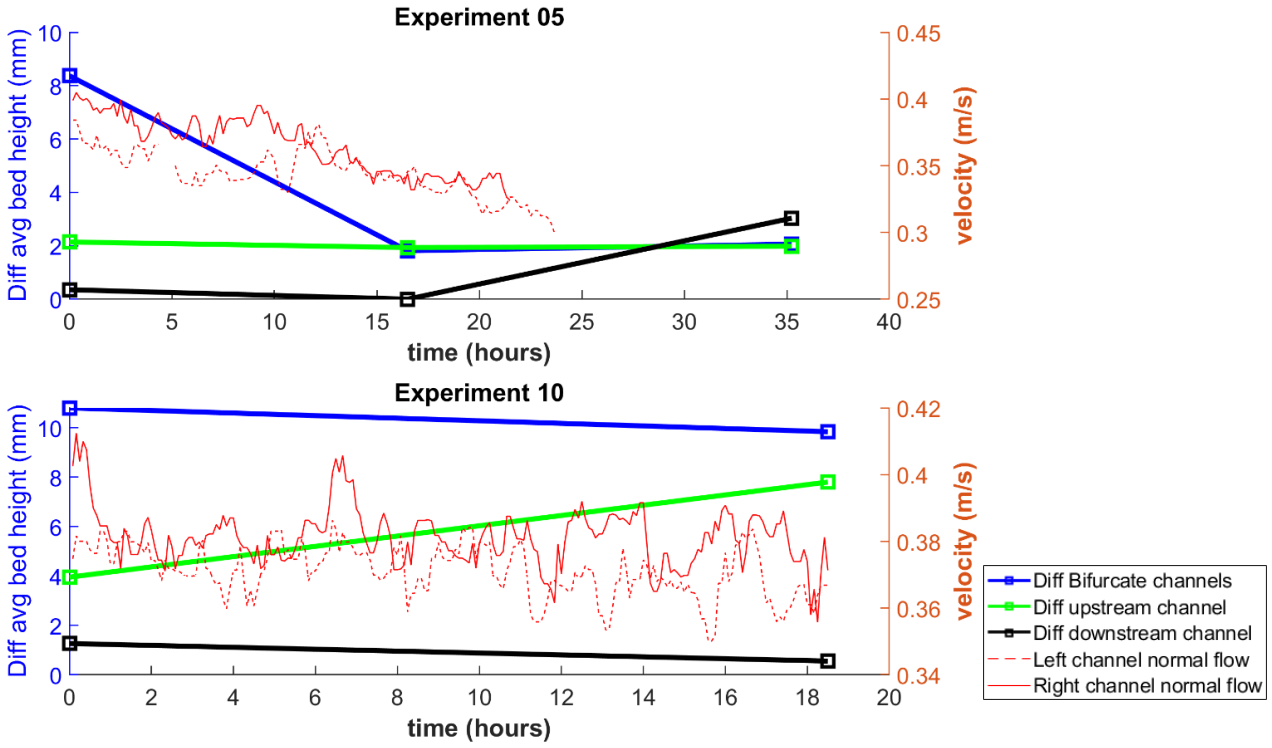

Figure 3.4 Reduced bed level and velocity timeseries for intermediate Shields stress, low width to depth ratio, hypothesized stable bifurcation, in experiment 5 and 10.

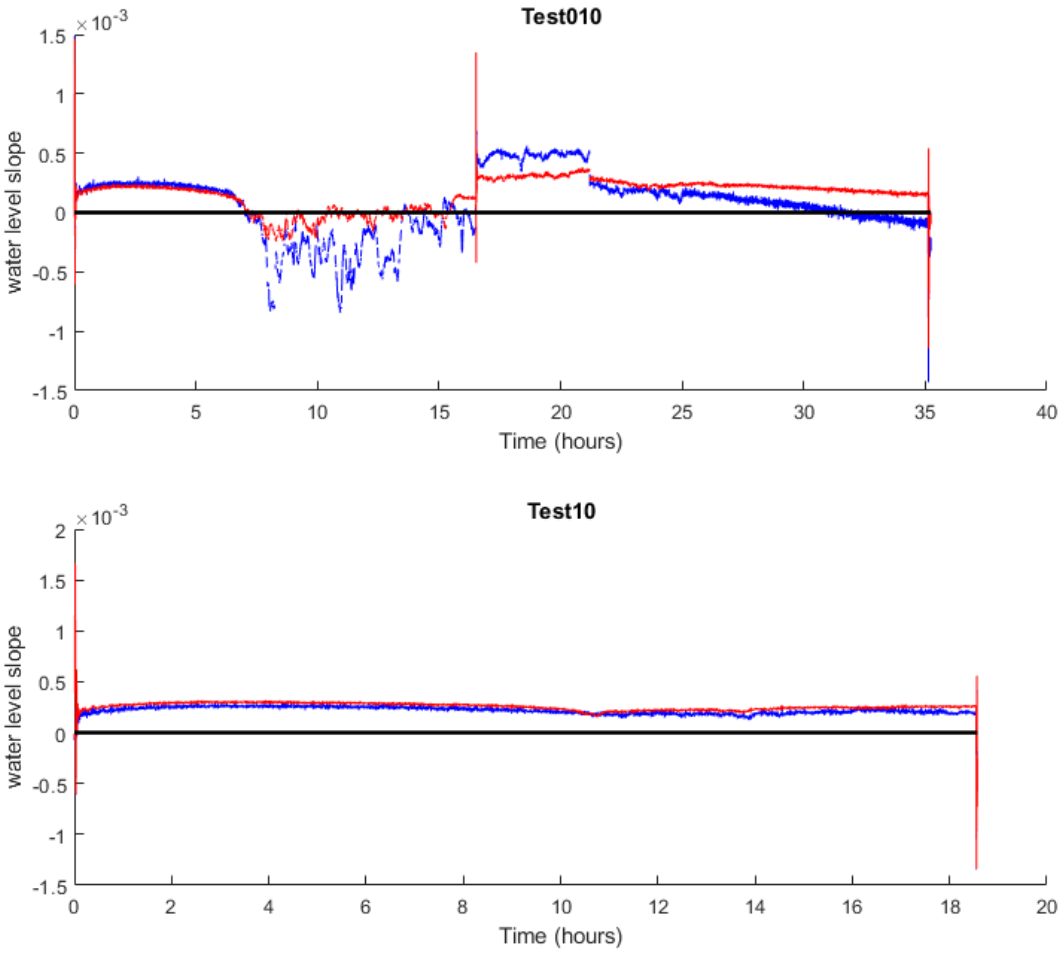

Figure 3.5 Water level slopes for intermediate Shields stress, low width to depth ratio, hypothesized stable bifurcation, in experiments 5 and 10. Red line is unperturbed channel blue line is perturbed channel.

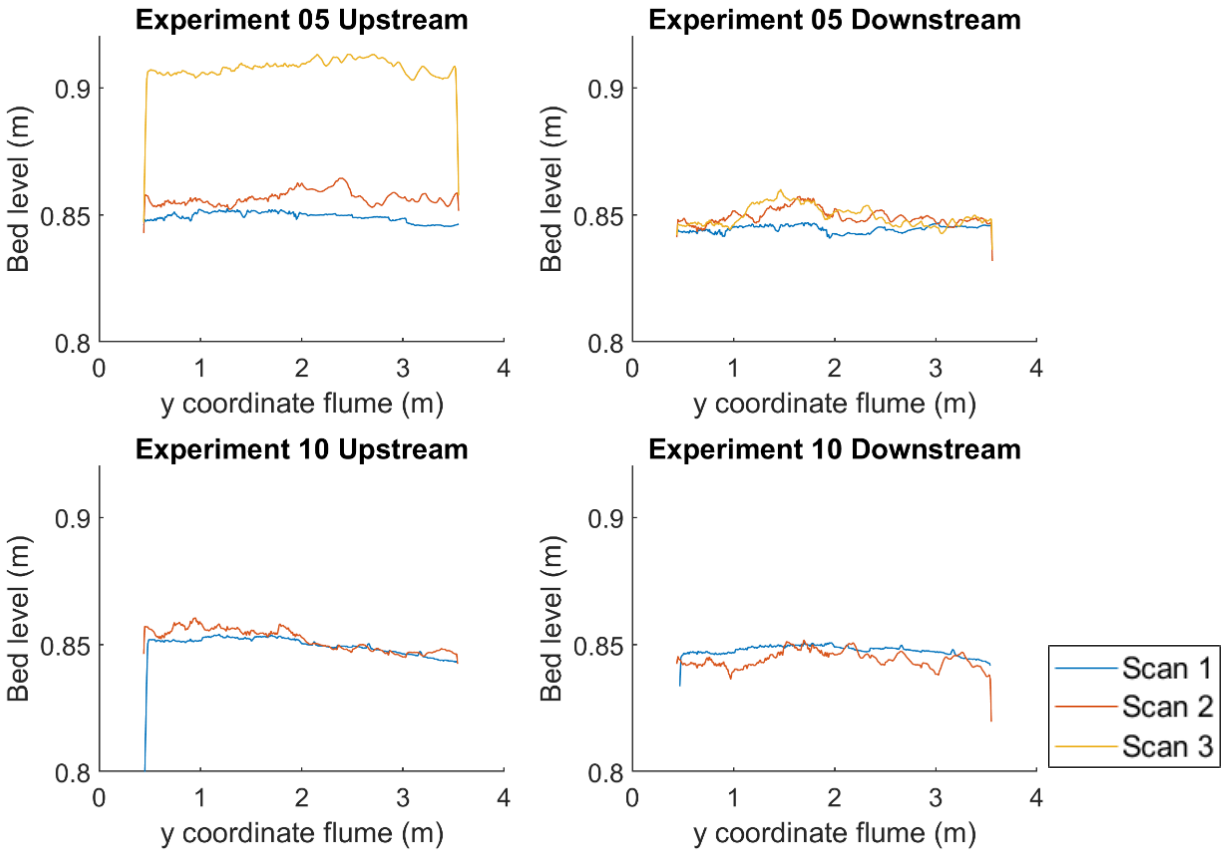

Figure 3.6 Average transverse bed levels for the up and downstream channels with intermediate Shields stress, low width to depth ratio, hypothesized stable bifurcation, in experiment 5 and 10. Flow direction was from high to low x coordinates (right to left).

3.2.2 Intermediate Shields stress high width to depth ratio, unstable bifurcation

Experiment 4 (high width depth ratio and intermediate mobility) in general showed a swift removal of the perturbation and increasing depth difference between the perturbed and unperturbed channels. Erosion of the unperturbed channel and aggradation of the section upstream of the perturbed channel were observed. Figure 3.7 shows the DEM results for the bathymetry of experiment 4. A slight error in the data for scan 1 should be ignored as it is caused by a bad scan run. The location and dimensions of the perturbations can still be made out. In the DEMs a pattern of sedimentation from x= 38 and higher and between y=0.5 and y=2.5 is observed, erosion of the bed can be seen to occur from x=35 all the way down the downstream part of the flume. These patterns of erosion and sedimentation indicate that the perturbed channel has a low transport capacity while the unperturbed channel has high transport capacity. The increasing depth of the unperturbed leads to an increase of the initial perturbation. The formation of a “bar” at the entrance of the perturbed channel slightly extends into the area in front of unperturbed channel. Erosion is strongest from the boundary wall towards the middle of the flume. The flow here seems to avoid the generated “bar”. The upstream channel in front of the unperturbed

channel initially remains relatively stable but then shows erosion over the last 3.5 hours of the experiment. Figure 3.8 shows the summarized bed level results and average velocity in both the channels. Here it can be observed that the difference in average bed height of the two channels increases in between the first two bed scans but slightly decreases over the final couple of hours of the experiment. The upstream and downstream channel however show a trend where there is deposition of sediment on the perturbed side of the channel. Examining the upstream channel shows that there is a strong preference of deposition in front of the perturbed channel resulting in an increasing difference between the bed level of upstream of the two channels. Looking at the downstream channel, both sides of the flume display erosion but the erosion at the unperturbed channel is much higher. The velocities in the experiment 4 show a divergent trend over time where the flow velocities were similar during the first 5 hours but then the velocities start to increase in the unperturbed channel. The velocities in the perturbed channel remain relatively stable over time. But a difference of 0.2 to 0.4 m/s can be observed around the end of the experiment. The deposition and erosion of the upstream and downstream channel can for a large part be explained through the hydraulic slope generated through the backwater effect. on closer inspection of the average transverse bed levels in figure 3.9, it becomes clear that over time a strong transverse slope is generated upstream of the bifurcation. The flat profile for y coordinates 0.5 to 2 in scan 1 is an average of that of the left side as an error in the scan data produced a saw blade pattern that should be flat. The figure also shows the increased erosion over the different scans leading to a stronger transverse slope. Looking at a similar figure of the situation downstream of the bifurcation it becomes visible that erosion on the unperturbed channel is relatively uniform and a small bed form appears to be formed just behind and close to the splitter plate on the side of the perturbed channel. This could possibly be caused by the relatively slower flow velocity and discharge from the perturbed channel locally reducing the transport capacity behind the confluence and thus inducing some sedimentation. It should be noticed that the bedform becomes smaller from the second to the final scan.

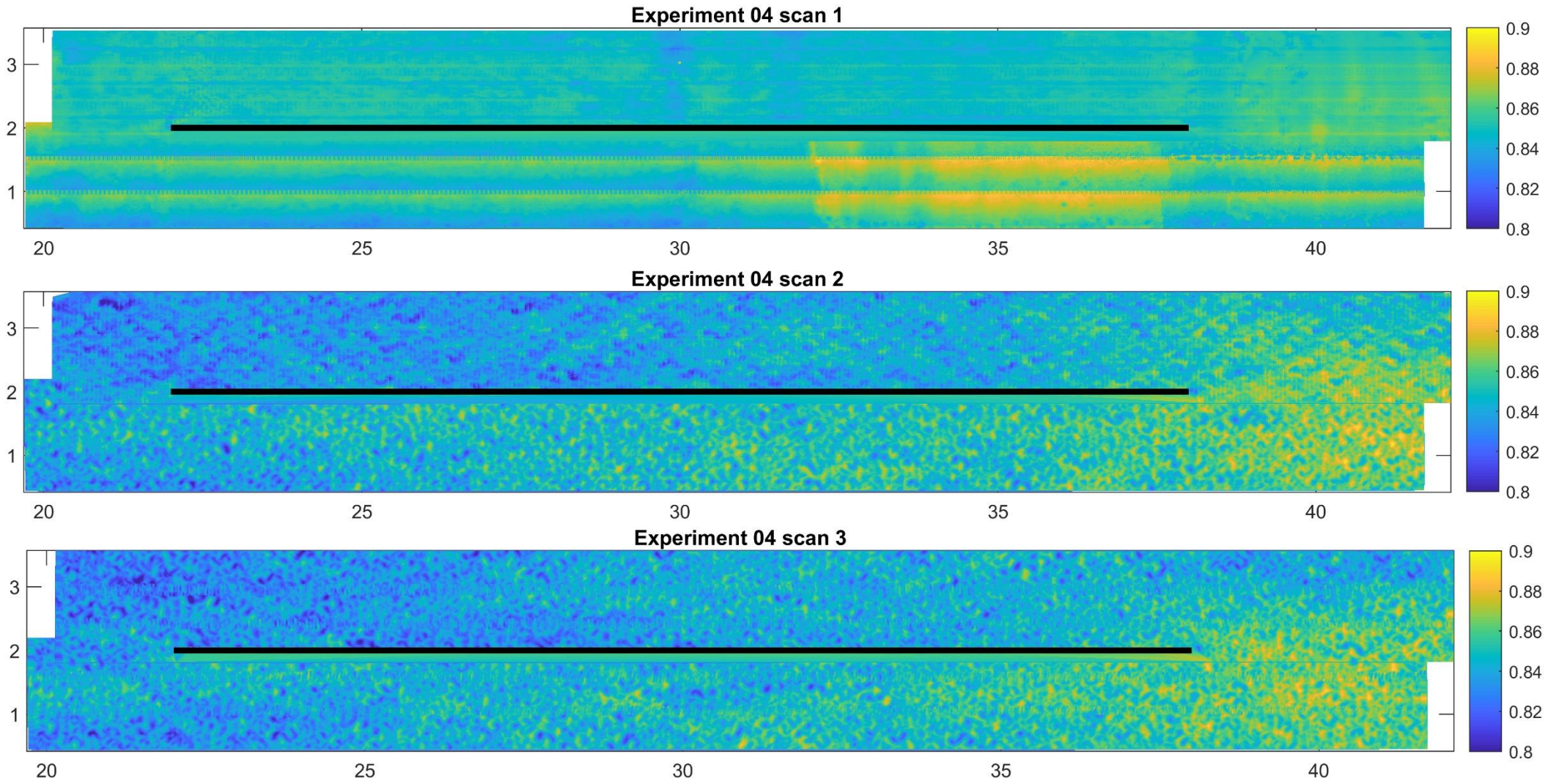

Figure 3.7 Digital elevation model for the different scans made for intermediate Shields stress, high width to depth ratio, hypothesized unstable bifurcation, in experiment 4. The black line shows the splitter plate location. X and Y axis are the flume coordinates in meters. Flow direction was from high to low x coordinates (right to left). Scan taken after: scan1 t=0h, scan 2 t=7.83h, scan 3 t=13h

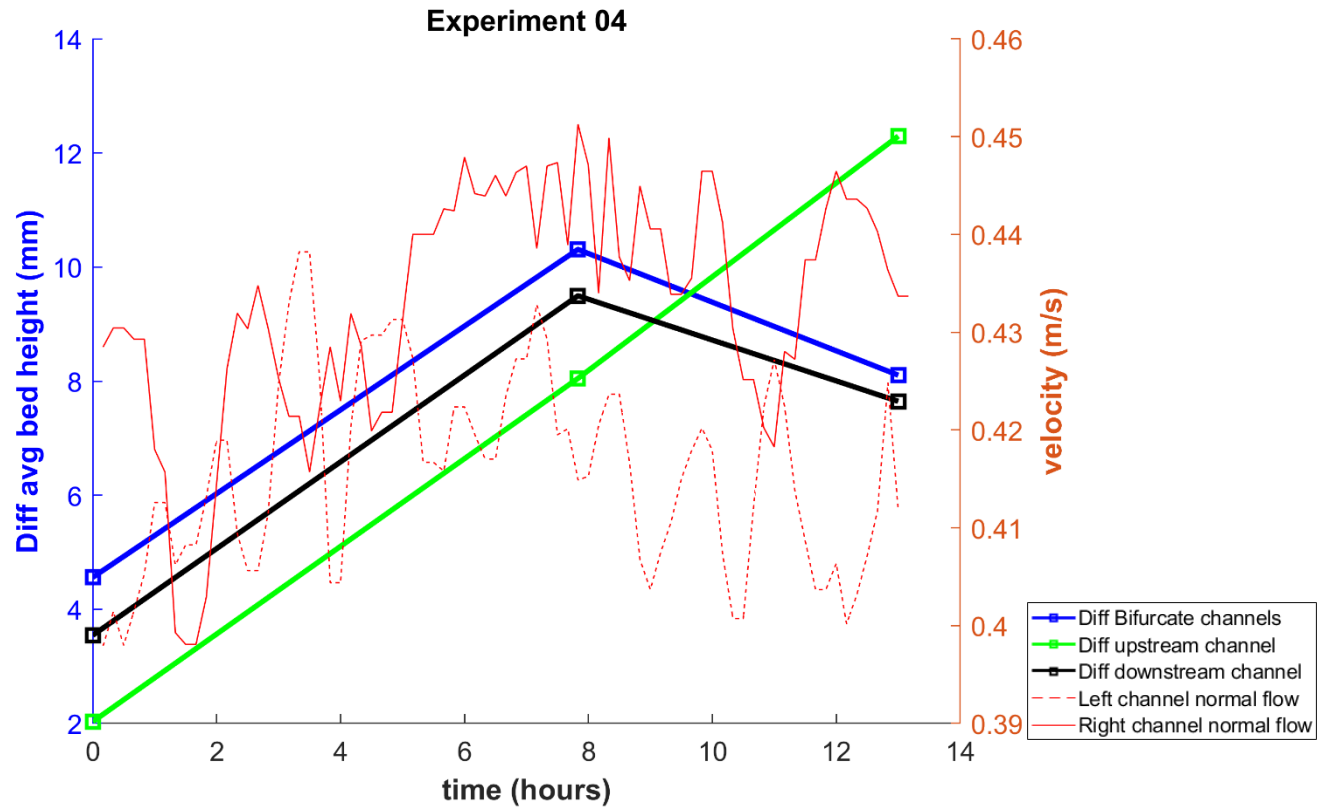

Figure 3.8 Reduced bed level and velocity data for intermediate Shields stress, high width to depth ratio, hypothesized unstable bifurcation, in experiment 4.

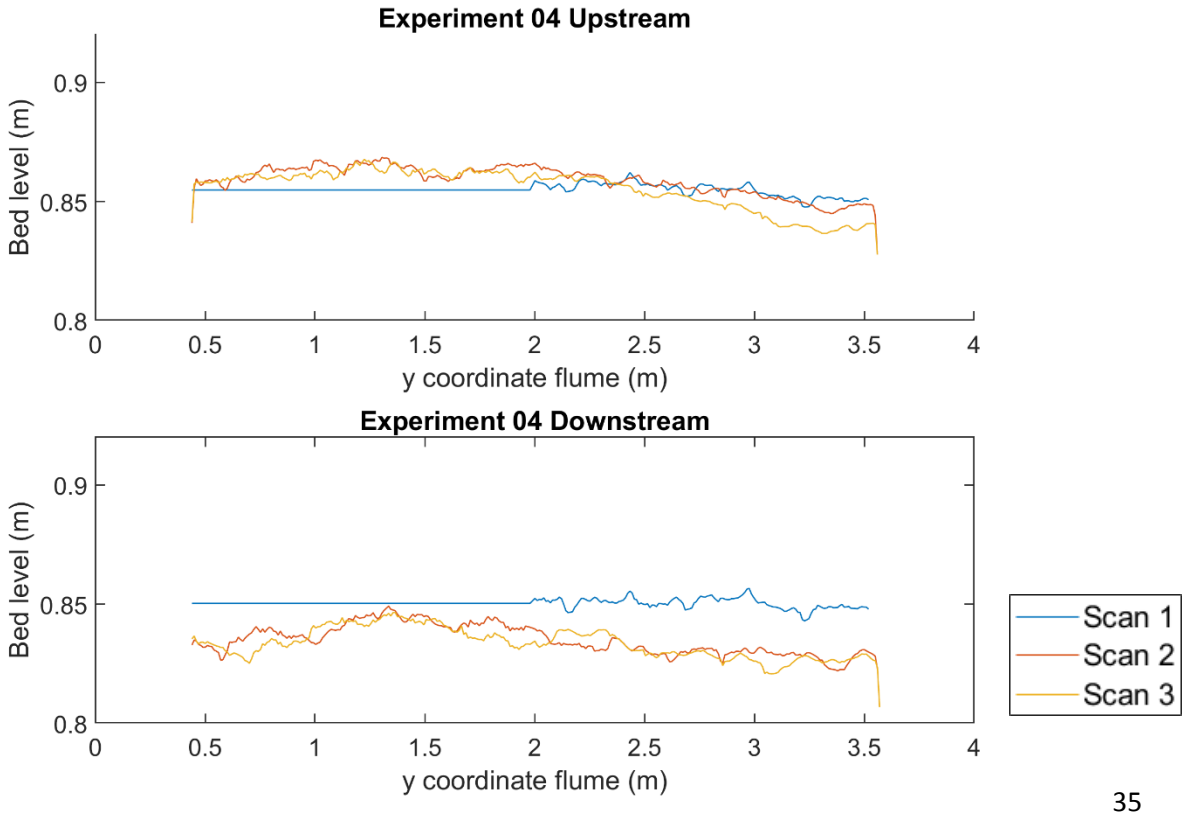

Figure 3.8 Average transverse bed levels for the up and downstream channels for intermediate Shields stress, high width to depth ratio, hypothesized unstable bifurcation, in experiment 4

3.2.3 High Shields stress low width to depth ratio, stable bifurcation.

Experiment 12 (low width depth ratio and high mobility) lead to general aggradation of the bed, and an average decrease in bed height between the two channels. The high erosion transport rate all over the flume, which caused of high levels erosion at the edge of the setup and run out of sediment input. For these reasons we have only been able to run two high Shields experiments and both for just a limited time (1 or 2 hours). Looking at the DEMs in figure 3.10 reveals that sedimentation takes place over the entire bed. The bedforms change from the tidally induced ripples and forms to what is best described as small dunes. The strong current transports sediment from upstream of the system into the system and causes aggradation in it as a whole. Scour can be observed at both ends of the splitter plate, while it does decrease over time in front of the splitter plate while increasing at the downstream side. Figure 3.11 shows the reduced bed level data for both experiment 9 and 12. Visible in this figure is that while the difference between the originally shallower channel and the deeper channel changes only very slightly during the first half our of testing during the last 25 minutes the difference decreases by a large margin on all sections. Especially the difference upstream of the bifurcation and between the channels decreases by multiple mm. Looking at experiment 12 it is hard to see a good trend in the velocities because of the limited amount of data points. This experiment was conducted on the final bed morphology of experiment 11 and while having a large difference initially the average bed elevation difference reduces towards the end of the experiment. During the first half hour of the experiment the differences between the two sides of the flume remain relatively stable. The slightly transverse slope, figure 3.12 that could be observed for the first scan entirely disappears in the duration of the experiment. A final important observation is that the originally shallower channel displays larger bedforms than the deeper channel. As such a deep dune trough and longer and higher dune crest are present in this channel while being absent in the other channel.

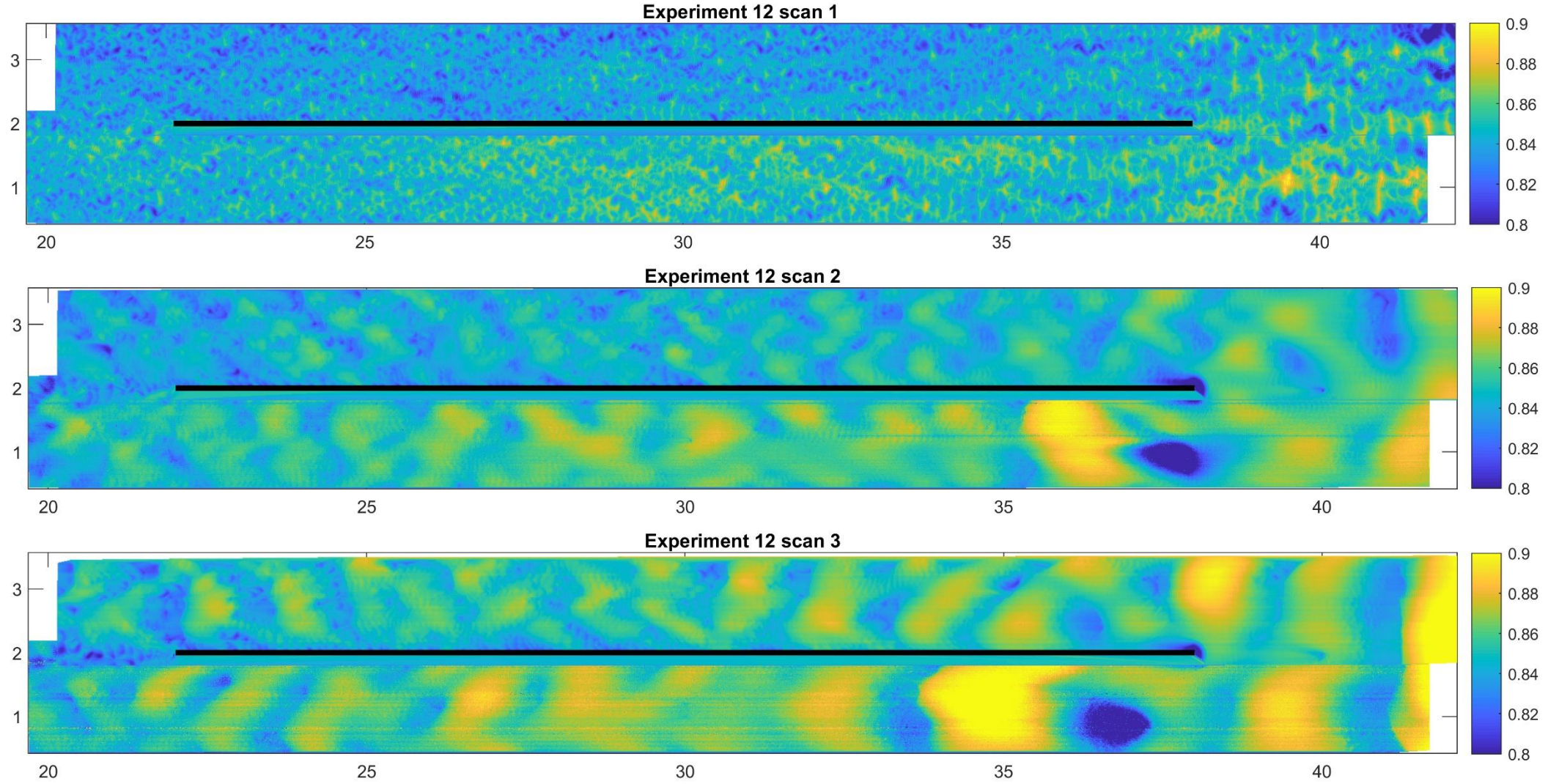

Figure 3.10 Digital elevation model for the different scans made for high Shields stress, low width to depth ratio, hypothesized stable bifurcation, in experiment 12. The black line shows the splitter plate location. X and Y axis are the flume coordinates in meters. Flow direction was from high to low x coordinates (right to left). Scan taken after: scan1 t=0h, scan 2 t=0.5h, scan 3 t=0.9h

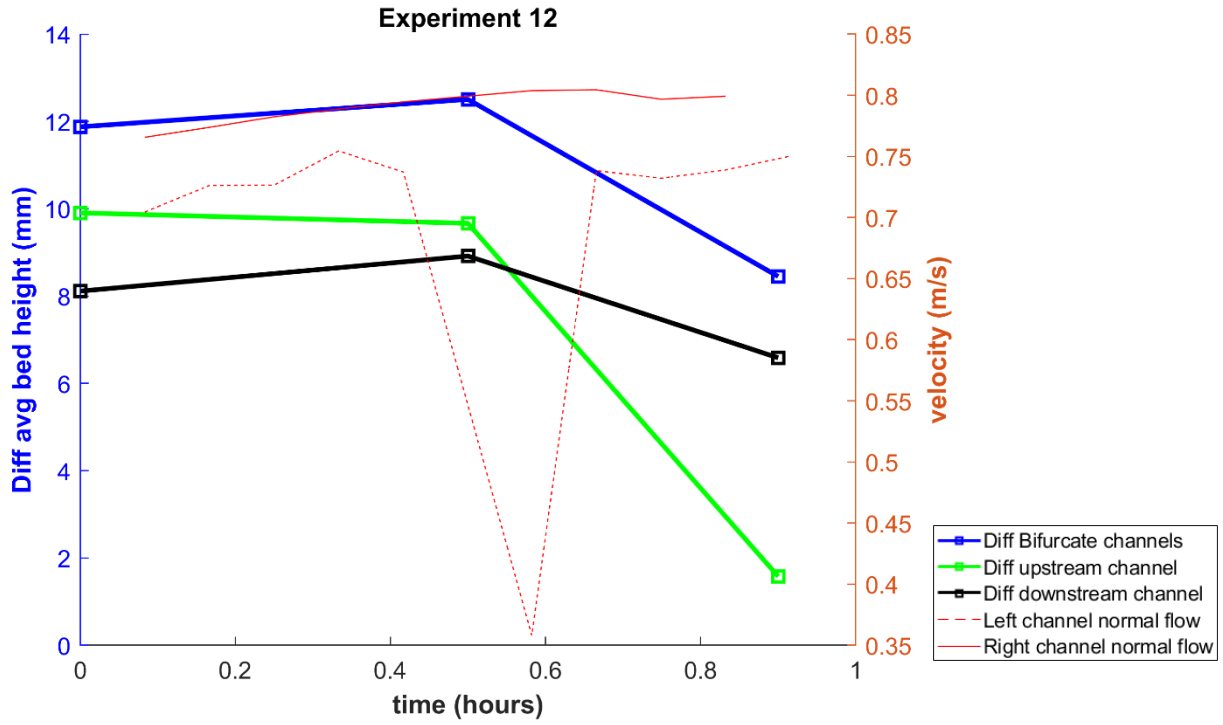

Figure 3.11 Reduced bed level and velocity data for high Shields stress, low width to depth ratio, hypothesized stable bifurcation, in experiment 12.

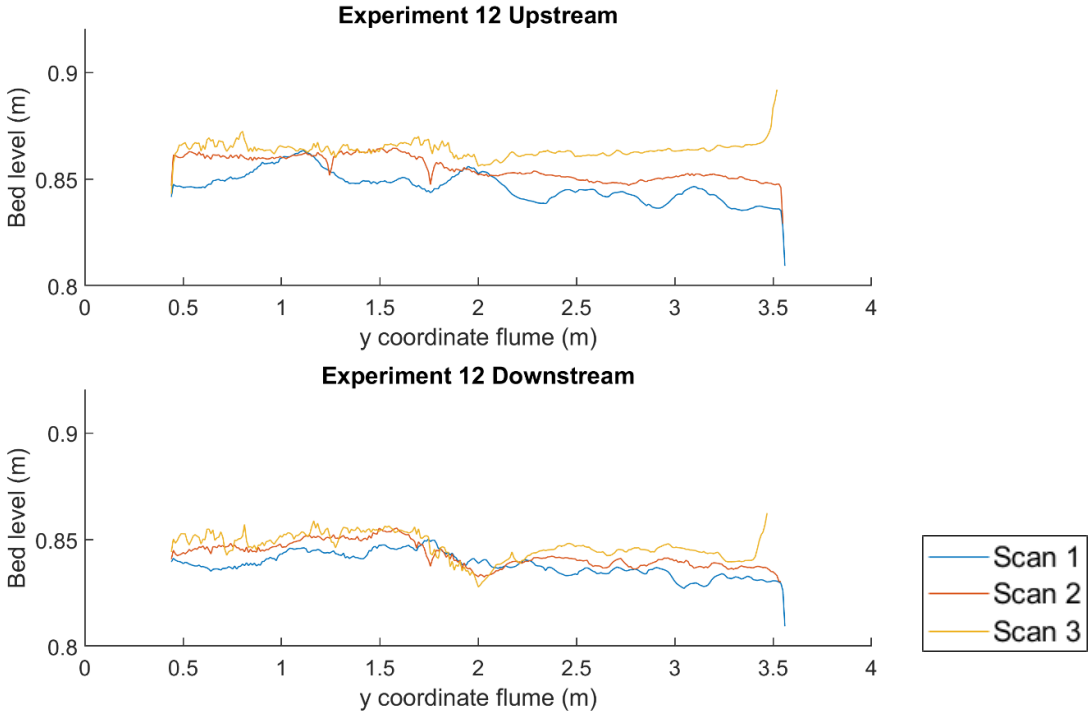

Figure 3.12 Average transverse bed levels for the up and downstream channels for high Shields stress, low width to depth ratio, hypothesized unstable bifurcation, in experiment 12

3.2.4 High Shields stress high width to depth ratio, unstable bifurcation.

Experiment 9 (high width depth ratio and high mobility) showed a swift removal of most of the perturbance and little depth difference between the two bifurcate channels but a strong scour upstream of the perturbation. The experiment was run for 2 hours in two periods of an hour. Figure 3.13 shows the DEMs produced for experiment 9. Looking at the morphology scour can be located in front of the bar in the opening of the bifurcate channel. A bit further upstream of the unperturbed channel another bar can be observed. Between the two bars a “channel” appears to have formed flowing from the scour into the unperturbed channel. During the first hour of running the experiment the difference between the perturbed channel and the unperturbed channel decreases as the bed morphology turns to a flat bed with only the formation of a couple of bars in against the splitter plate and the outside flume wall (figure 3.11). During the first scan these are best observed around and upstream of the splitter plate. During the second leg of the experiment a change in velocity can be observed in the vectrino data, that suggests a change in discharge division over the two channels, but faster velocities in the perturbed channel were only observed for about 30 minutes until the vectrino results return to a more similar trend as observed in the first leg of the experiment. In this time the difference in average bed level slightly increase for the bifurcate channels and downstream of the splitter plate. Because of the short run time of the experiment it is however again hard to properly analyse the vectrino results. Upstream of the splitter plate however the difference drastically increases up to 23mm because of the big scour being developed in front of the perturbed channel. Figure 3.12 shows that while over the 3 scans a strong slope is formed this slope is surprisingly directed towards the perturbed channel and not towards the initially deeper channel.

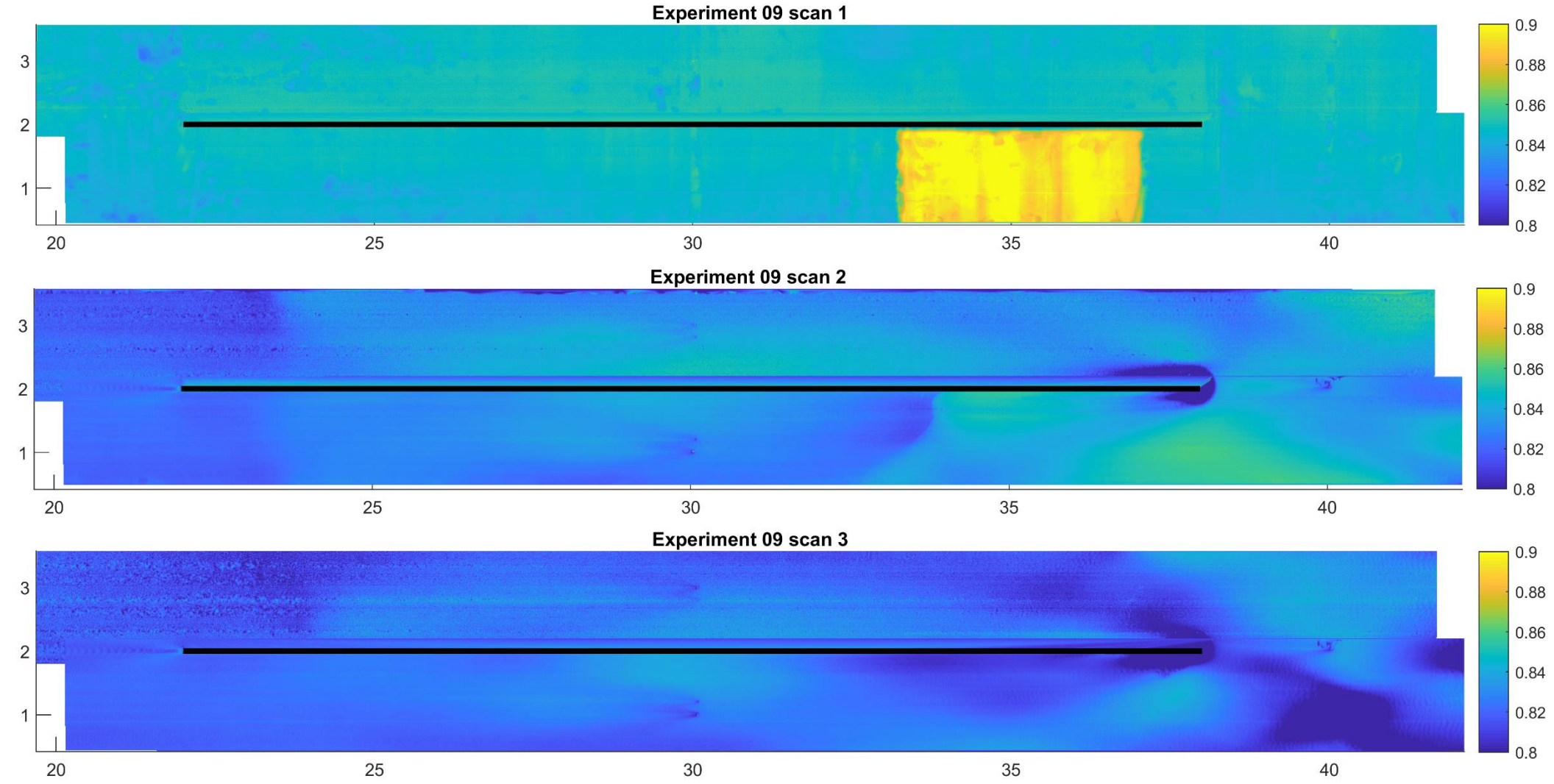

Figure 3.13 Digital elevation model for the different scans made for high Shields stress, high width to depth ratio, hypothesized unstable bifurcation, in experiment 9. The black line shows the splitter plate location. X and Y axis are the flume coordinates in meters. Flow direction was from high to low x coordinates (right to left). Scan taken after: scan1 t=0h, scan 2 t=1.16h, scan 3 t=2.22h

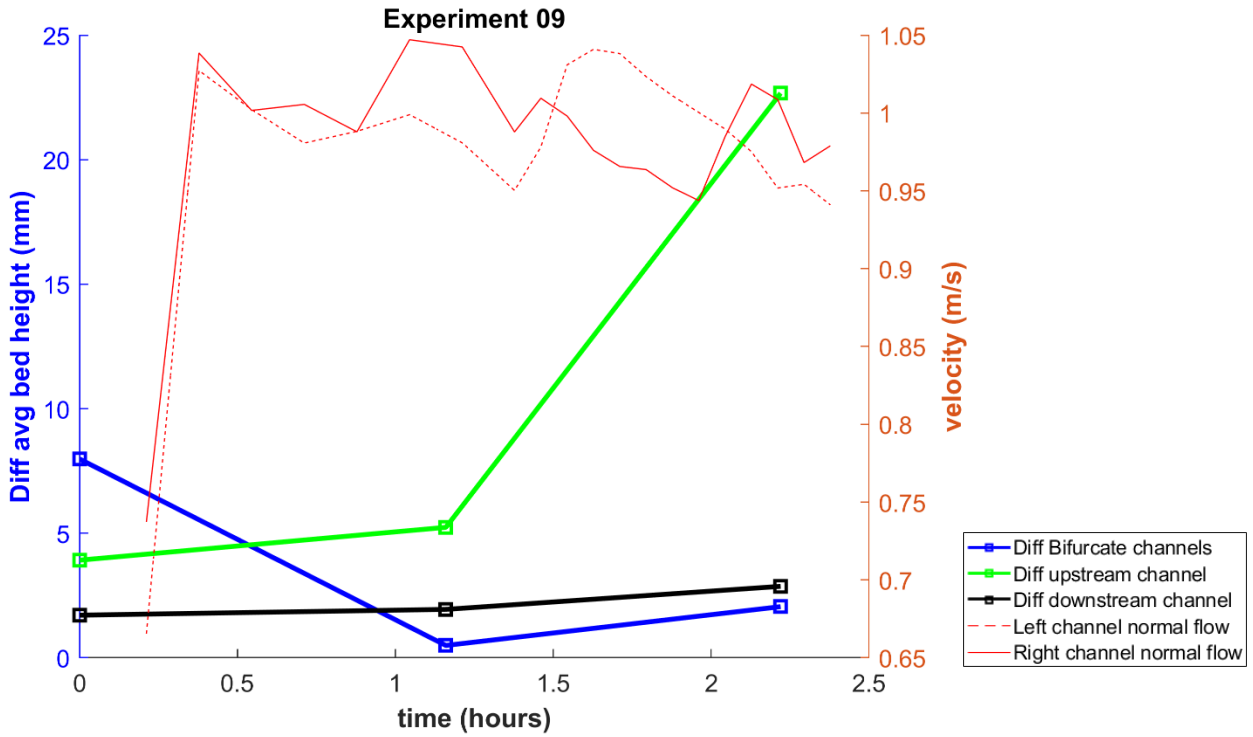

Figure 3.16 Reduced bed level and velocity data for high Shields stress, high width to depth ratio, hypothesized unstable bifurcation, in experiment 9.

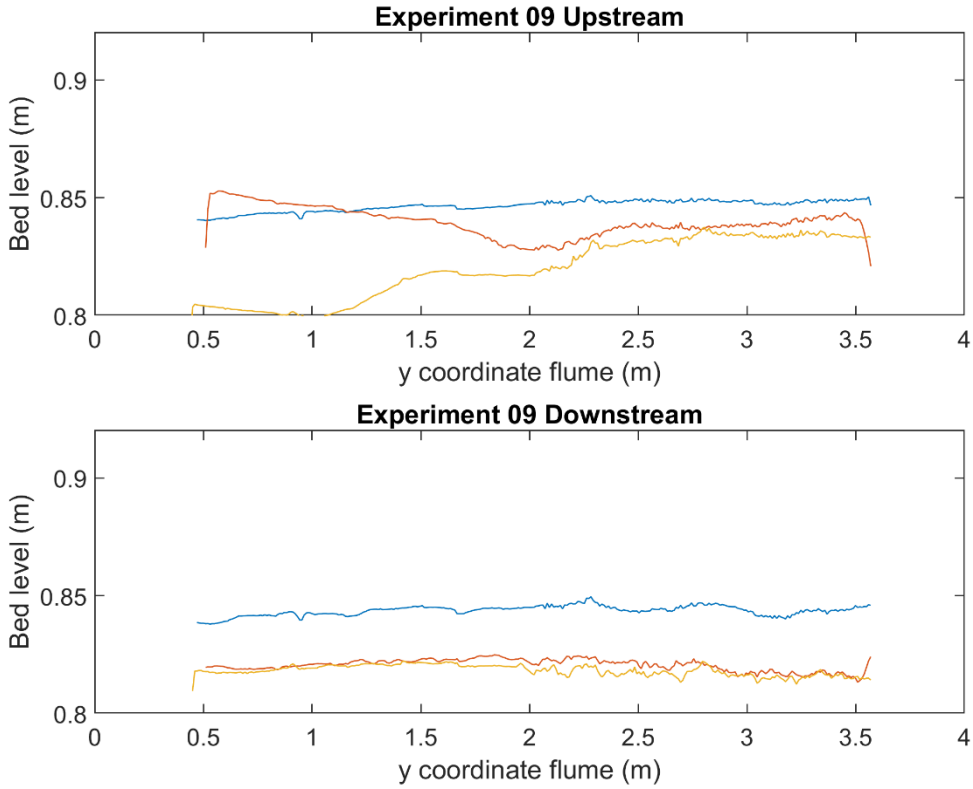

Figure 3.15 Average transverse bed levels for the up and downstream channels for high Shields stress, high width to depth ratio, hypothesized unstable bifurcation, in experiment 9.

3.3 Tidal experiments

3.3.1 Intermediate Shields stress low width to depth ratio, stable bifurcation.

Experiment 6 and 8 (low width depth ratio and intermediate mobility and reversing flows) generally showed a slow removal of the perturbation and a slow reduction in depth difference between the perturbed and unperturbed channel. Both up- and downstream channels show no erosional or depositional trends. Differences between experiment 6 and 8 thus appear to be caused by the different initial situations, but they do display similar morphological features and development. The two experiments are duplicates except for the initial bed. Where a perturbation was induced in experiment 6 the initial bed of experiment 8 is the final bed morphology of experiment 7 as can be seen in the DEMs (figure 3.14 and figure 3.15). Over the 3 scans made for experiment 6 a decrease in difference between the average bed level can be observed for the bifurcate channels and the downstream channel (figure 3.16). The upstream channel does however see an increase in the difference between the left and right channel. It should be noted that this increase in difference is caused by the formation of a small bar in front of the unperturbed channel, as seen in figure 3.17. This figure, except for the bar, does not show a clear transverse slope in either direction in both the upstream and downstream situation. The figure does show the interesting formation of bed forms perpendicular to the flow. While some longer lateral ripples can be observed most of them are cut through by the deeper “snake like” erosions, figure 3.14. These bedforms are found throughout the entirety of the bed and in both experiments, though less pronounced on the location of the original perturbation. Over time the formations can be seen to be relatively stable in size, as observed from the difference between the second scan and third scan for experiment 6.

Experiment 8 dealt with a larger difference between the two bifurcate channels but over time does show a trend where the difference reduces, if only by a small margin. The difference at the up and downstream parts of the bed however slightly increased over time, from about 3 mm to about 4 mm. The vectrino data unlike in experiment 6 appears not to be as equal. While flow in both directions results in similar flow velocities in experiment 6 the flow velocities for flow in the normal direction is lower than the flow velocities in reverse flow in experiment 8. A difference between the two channels cannot really be discerned. Preferential flow for either of the two flow direction was not observed for these experiments. Looking at the transverse bed elevations (figure 3.17) a similar pattern forms as in experiment 6, where small bars seem to form on the unperturbed channel side and there is no clear transverse slope. Of interest for this experiment is that it started with the bed morphology of a high width to depth ratio experiment, which has its own specific bed morphology features as will be discussed below and ended up having comparable bed morphology to experiment 6 that started from a flat bed with a perturbation.

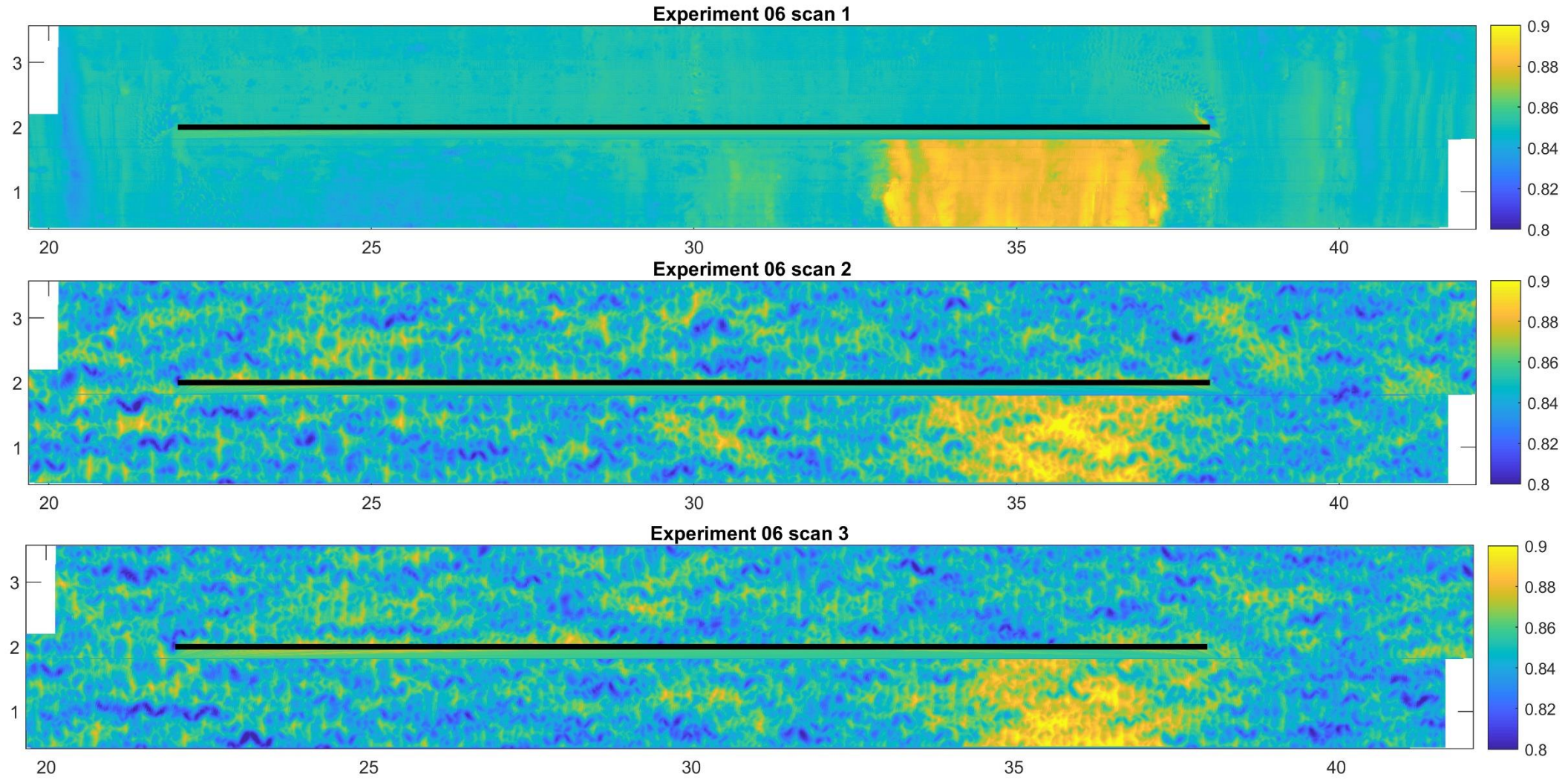

Figure 3.16 Digital elevation model for the different scans made for intermediate Shields stress, low width to depth ratio and reversing flow, hypothesized unstable bifurcation, in experiment 6. The black line shows the splitter plate location. X and Y axis are the flume coordinates in meters. Flow direction were reversing from right to left and left to right. Scan taken after: scan1 t=0h, scan 2 t=12h, scan 3 t=18h

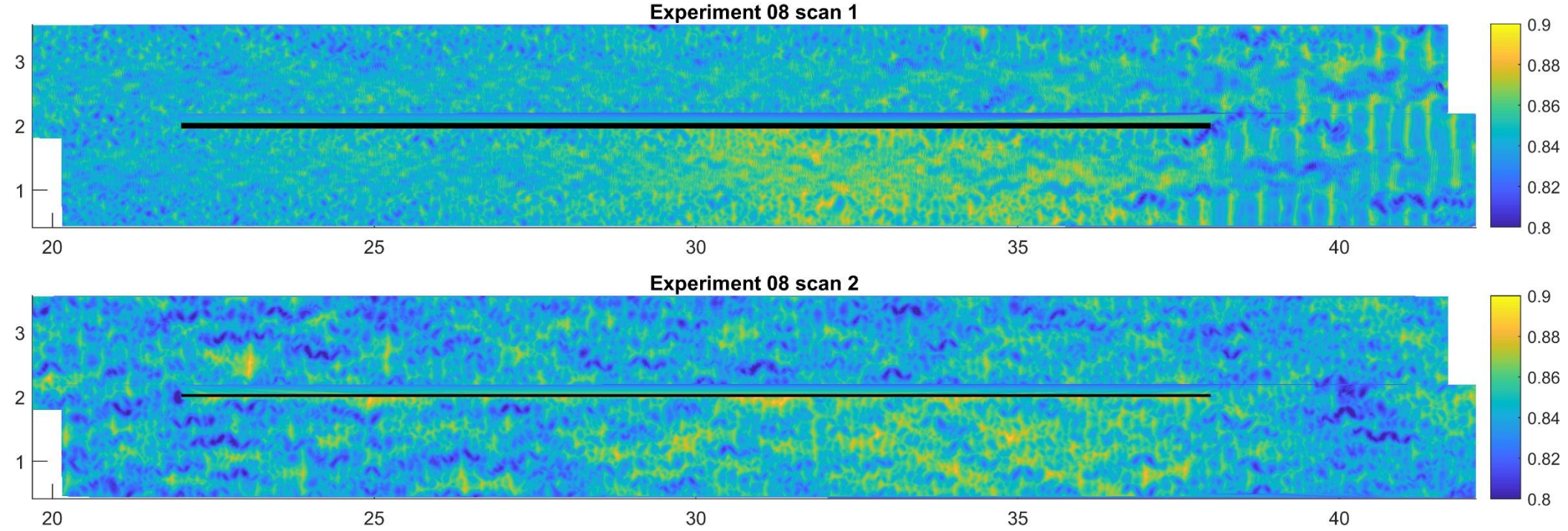

Figure 3.27 Digital elevation model for the different scans made for intermediate Shields stress, low width to depth ratio and reversing flow, hypothesized unstable bifurcation, in experiment 5. The black line shows the splitter plate location. X and Y axis are the flume coordinates in meters. Flow direction were reversing from right to left and left to right. Scan taken after: scan1 t=0h, scan 2 t=19.58h

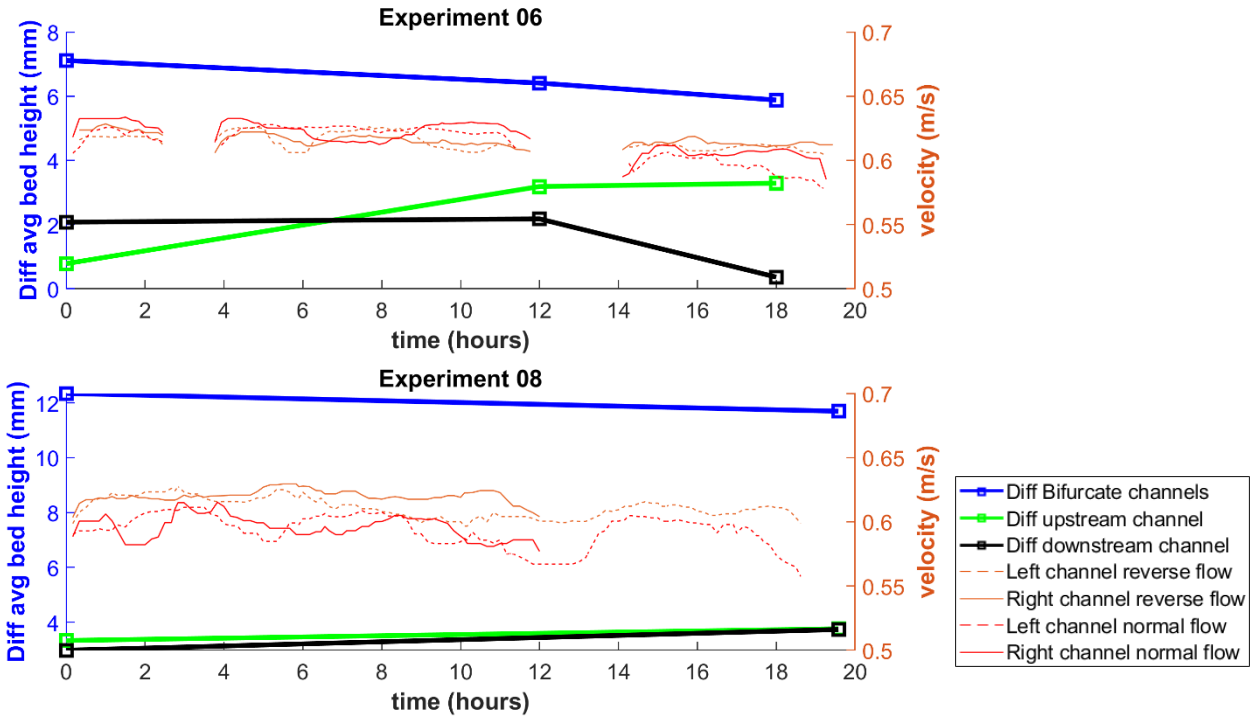

Figure 3.18 Reduced bed level and velocity data for intermediate Shields stress, low width to depth ratio and reversing flow, hypothesized unstable bifurcation, in experiment 6 and 8.

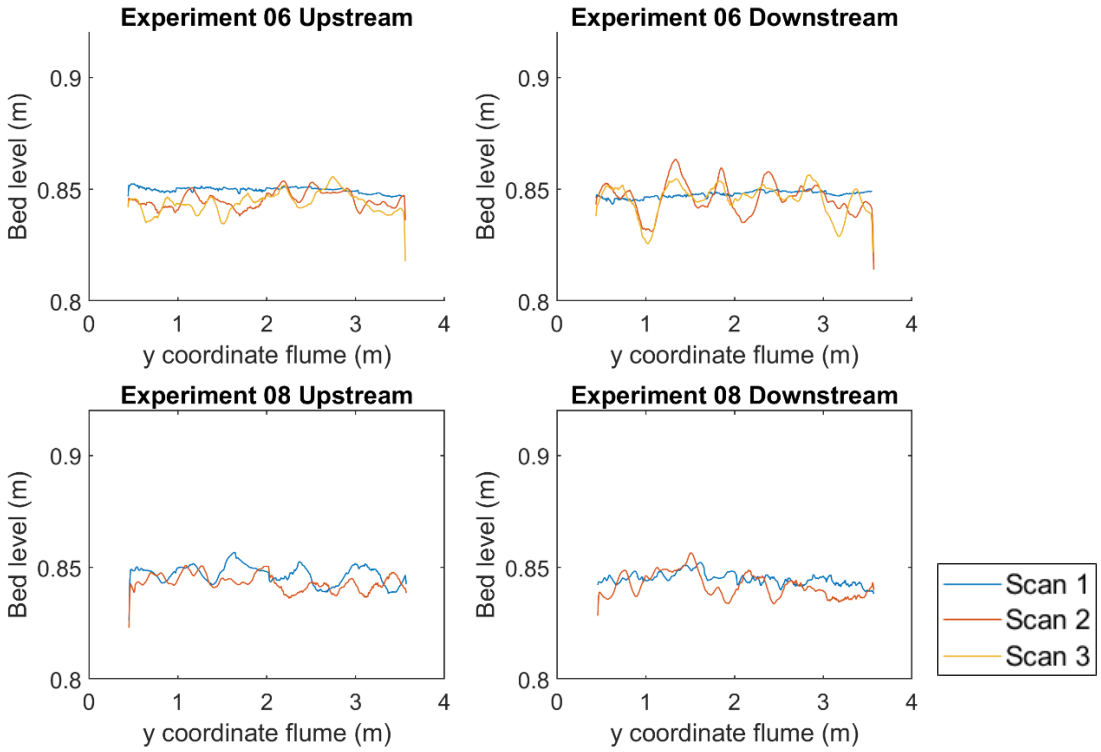

Figure 3.3 Average transverse bed levels for the up and downstream channels for intermediate Shields stress, low width to depth ratio and reversing flow, hypothesized unstable bifurcation, in experiment 6 and 8.

3.3.2 Intermediate Shields stress high width to depth ratio, stable bifurcation.

Experiment 7 and 11 (low width depth ratio and intermediate mobility and reversing flows) generally showed a decrease of the perturbation and increasing depth difference between the perturbed and unperturbed channels. Erosion of the unperturbed channel and aggradation and evolution of distinct bedforms in the section upstream of the perturbed channel were observed.
These experiments are also duplicates except for the initial bed. Where a perturbation was induced on a flat bed in experiment 7 the initial bed of experiment 11 is the final bed morphology of experiment 11 (figure 3.18 and 3.19). The difference in average bed level between the two bifurcate channels slightly increases in both experiment 7 and 11 (figure 3.20). And while the average difference in bed level of the upstream part also increases in both experiments it decreases in the downstream part for experiment 7 while it increases quite drastically for experiment 11. The vectrino results of these experiments show an interesting difference when comparing the direction of flow. While flow reaches velocities above 0.5 and 0.4 m/s in both channels under normal flow conditions for experiment 7 and 11 respectively, velocities measured for reverse flow are at least twice as low. This is however most likely caused by the different water surface slope and the water depth at which the vectrinos thus actually measured velocities. For as far as there are measurements in both the channels it can also be observed that the flow velocities in both the channels diverge, indicating a difference of discharge in both the channels. What is noteworthy is that the difference between the two channels is larger for the reverse flow and interestingly enough the unperturbed channel velocities are lower than the perturbed channel flows. During normal flow however the unperturbed channel experiences higher velocities. Looking at figure 3.21 the transverse

bed levels of experiment 7 shows the formation of bed structures but relatively very little erosion of the bed both upstream and downstream of the splitter plate. Experiment 11 displays more interesting results with the formation of a slight transverse bed slope. Though it should also be noticed that the initial bed already has a very slight slope, it does display an increase in slope over time. The downstream transverse bed level displays erosion in the unperturbed channel while there is some sedimentation around the area of the confluence of the flows.

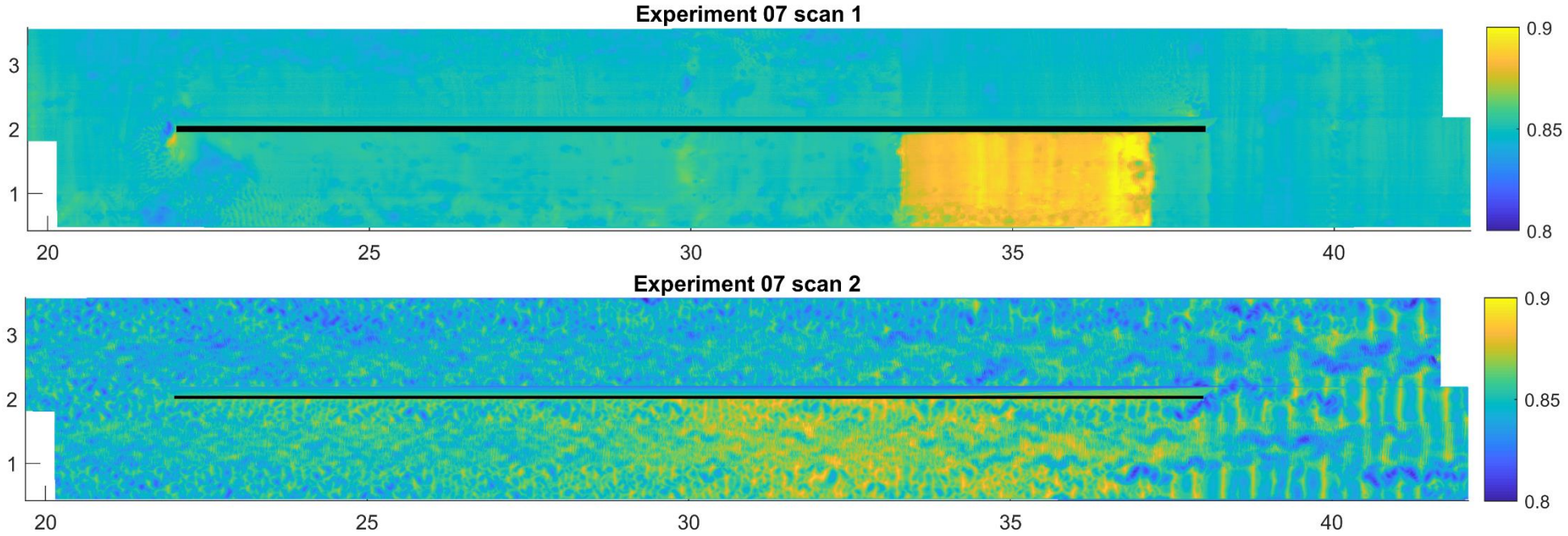

Figure 3.20 Digital elevation model for the different scans made for intermediate Shields stress, high width to depth ratio and reversing flow, hypothesized unstable bifurcation, in experiment 7. The black line shows the splitter plate location. X and Y axis are the flume coordinates in meters. Flow direction were reversing from right to left and left to right. Scan taken after: scan1 t=0h, scan 2 t=18.47h

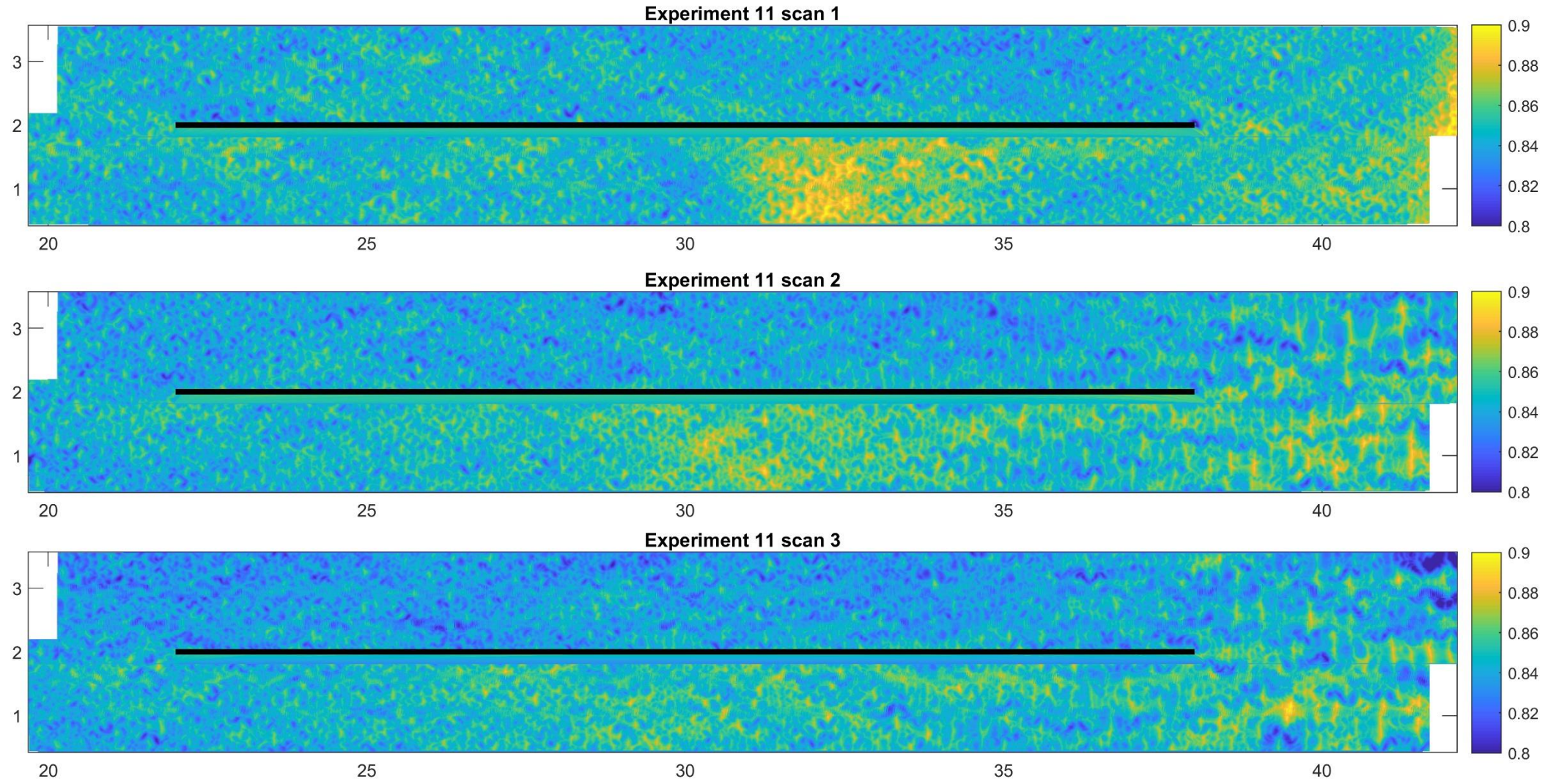

Figure 3.21 Digital elevation model for the different scans made for intermediate Shields stress, high width to depth ratio and reversing flow, hypothesized unstable bifurcation, in experiment 11. The black line shows the splitter plate location. X and Y axis are the flume coordinates in meters. Flow direction were reversing from right to left and left to right. Scan taken after: scan1 t=0h, scan 2 t=18h, scan 3 t=38h

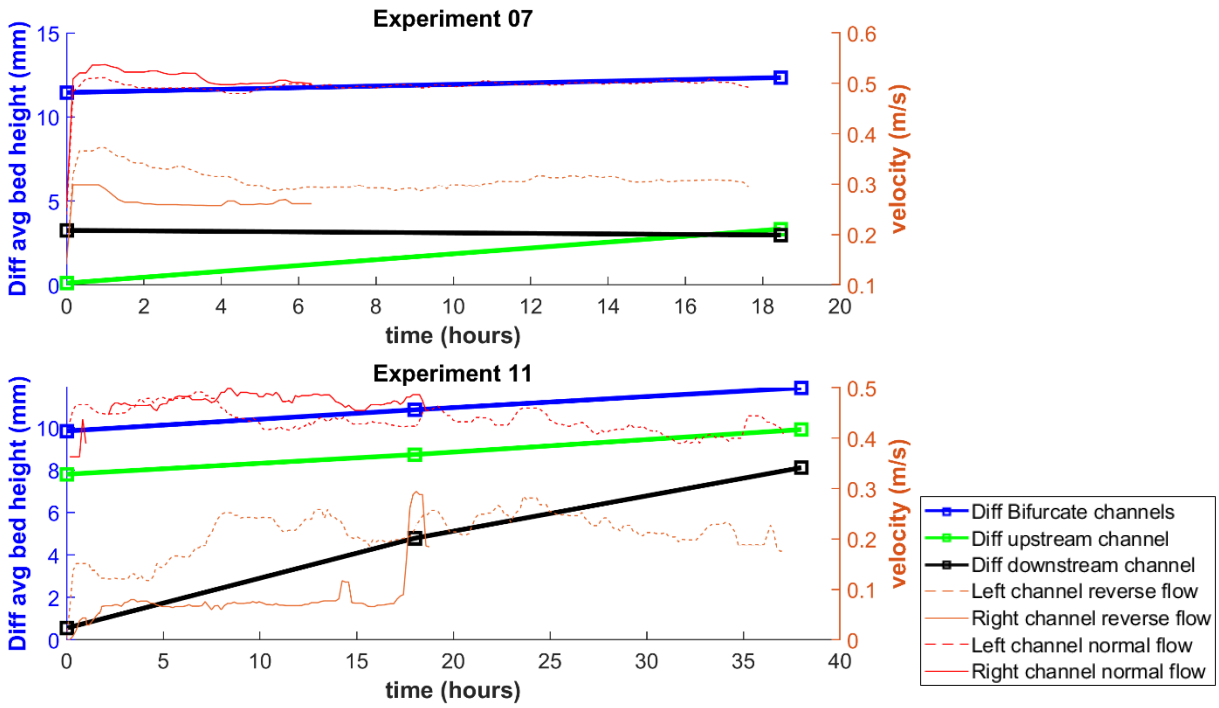

Figure 3.22 Reduced bed level and velocity data for intermediate Shields stress, high width to depth ratio and reversing flow, hypothesized unstable bifurcation, in experiment 7 and 11.

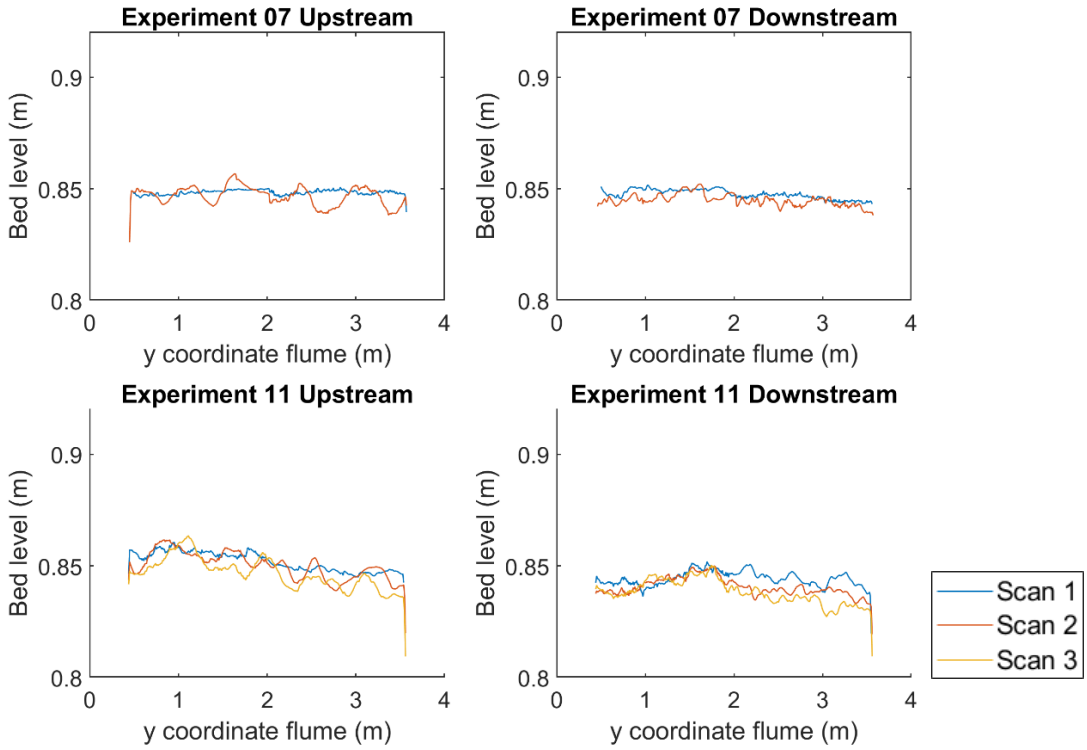

Figure 3.23 Average transverse bed levels for the up and downstream channels for intermediate Shields stress, high width to depth ratio and reversing flow, hypothesized unstable bifurcation, in experiment 7 and 11

3.4 Model Results

Model results provide similar trends in morphological change for the test setup, resulting in unstable bifurcations for high width to depth ratios and stable bifurcations for high width to depth ratios. 1D nodal point models were run to simulate the results as observed in the experimental setup and presented in the figures below. The average transverse bed elevation resulting from the experiments (figure 3.1) and from the models (figure 3.24) for both sides of the flume were plotted. These show that with exception of the formation of bedforms the bed levels of the experiments follow the same trends over time as the models. Unidirectional flow at a high width to depth ratio results in a strong bed slope and a fast erosion of the perturbation. The discharge difference between the two channels however will cause the unperturbed channel to erode deeper than the perturbed channel. Unidirectional flow at a low width to depth ratio will slowly transport the perturbation downstream, but the difference between the two channels is much smaller. The tidal experiments at high width to depth ratios will produce a very slight bed slope and erode the perturbation similarly to the unidirectional situation. A strong difference between the perturbed and unperturbed channel is observed again, where the unperturbed channel erodes deeper than the perturbed channel. The modelled tidal low width to depth ratio results show that similar to the unidirectional model, with the same geometry and mobility the perturbation erodes rather slowly, with the exception that while there was migration of the perturbation in the unidirectional case the perturbation is almost immobile in the tidal experiment. The difference in bed level between

the two different channels is relatively small, similar to the unidirectional results, with the exception of where the perturbation is still present.

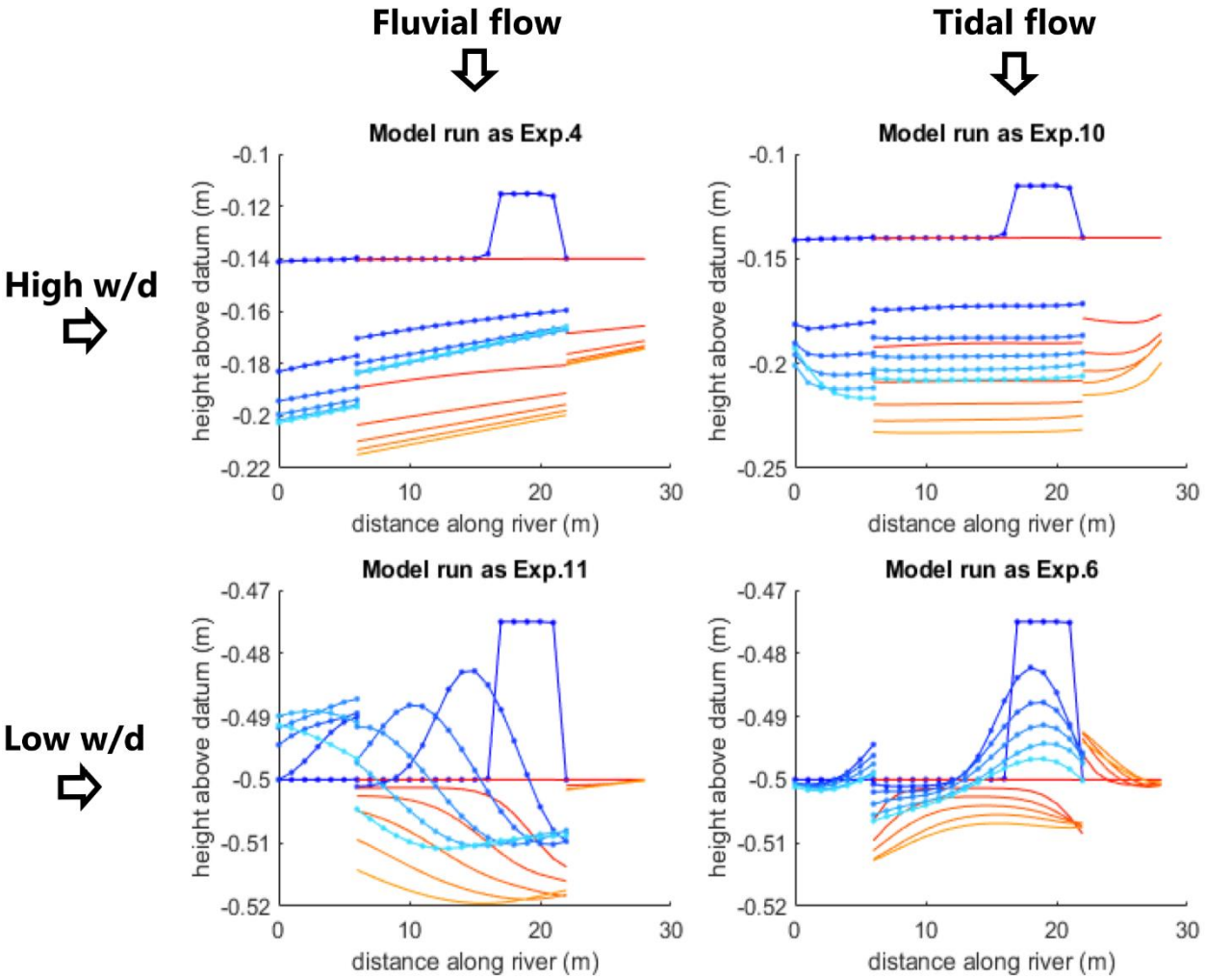

Figure 3.24 Bed evolution over time for the model runs, evolution illustrated from dark blue and red to orange and light blue. It can be observed that there is a larger difference between the bed elevation for experiments with high width to depth ratios than for experiments with low width to depth ratios. The effect of the tidal flow is mainly that little to no bed slope evolves and there is migration of the perturbation as visible for the model run of experiment 6.

In Figure 3.25 a comparison between model and the experiments is plotted the differences between the two channels for each case . From this figure it can be observed that the difference between the bifurcate channel increases for both model and experimental results increase for high width to depth ratios and decrease for low width to depth ratios. There is however differences visible in the modelled results and the experimental results for the low width to depth ratio experiments. It should also be noticed that a lot of change happens in the first timestep for the model results. This is most likely related to the “warm up” of the model before predicting change accurately.

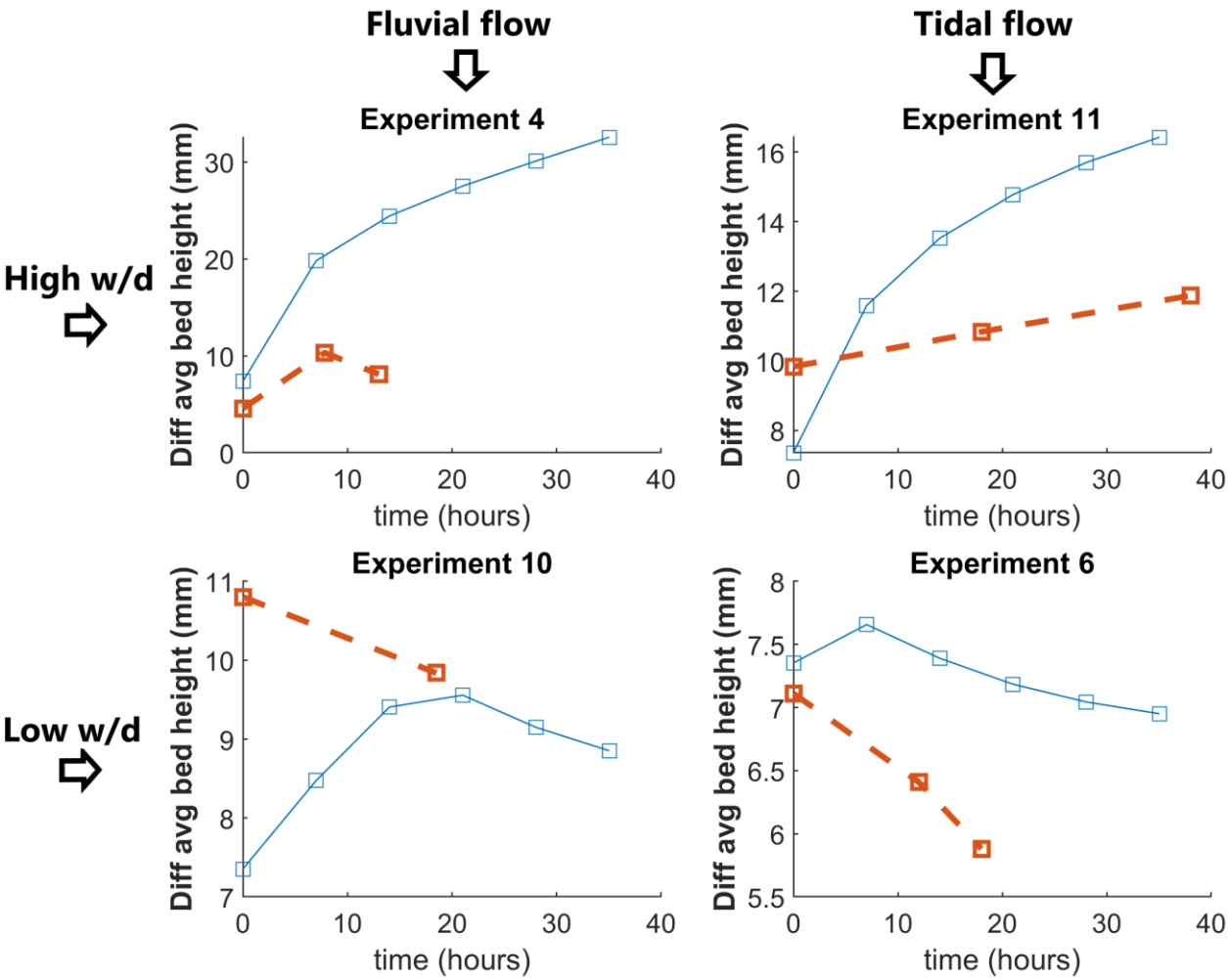

Figure 3.25 Measured and modelled evolution of bed height difference between the perturbed and unperturbed channel, in red and blue respectively. From these figures it can be observed that in both the model and the measured results there is an overall reduction of the difference between the bed height for low width to depth ratios and an increase in difference in bed height for high width to depth ratios. The influence of the reversing tidal flows is the reduction of the speed at which this reduction of the speed at which these evolutions take place.

4 Discussion

4.1 Stability

After analyzing all the results it can be concluded that there is a relationship between the width to depth ratio of the upstream channel and the stability of the bifurcation. As influences caused by bends in the flow or erodible banks were removed from these experiments, to isolate the effects of the sediment mobility and width to depth ratio, the transverse slope effect should be the only sediment redistributing mechanism affecting the setup. Under these conditions bifurcations will thus evolve into a stable symmetrical bifurcation when the upstream channel has a low width to depth ratio and evolve into a unstable asymmetrical bifurcation when the upstream channel has a high width to depth ratio. The high mobility experiments also showed the expected behaviour as predicted by the BRT model, as displayed in figure 1.3. The experiments were plotted in a stability diagram plot (figure 4.1) with Shields mobility plotted against the width to depth ratios of the executed experiments. Unidirectional experiments are denoted as red squares and where they landed in the plot coincided with their stabilizing or destabilizing behavior as discussed in the results section above. Tidal experiments exhibit the same stable and unstable behaviour dependent on the width to depth ratio of the upstream (and downstream) channel. When comparing this figure with previous research (figure 1.3), the addition of lower width to depth ratios and higher mobility values should be noted. The unidirectional results, as discussed in the results section, showed a clear difference between higher and lower width to depth ratios. Where a clear trend for a decreasing difference between the two bifurcate channels was observed for the high width to depth experiments the opposite, with increasing differences, could clearly be discerned for the low width to depth ratios. Including the morphological formation of larger transverse bed slopes for the higher width to depth ratios the difference between the two bifurcate channels increased over time. The experiments in this research experienced the strongest formation of transverse bed slopes at experiments with high width to depth ratios. The formation of such transverse bed slopes at these geometries is in accordance with the data found by Baar et al. (2017). Previous research on bifurcations through models has already isolated the importance of the geometry of the two channels (Wang et al., 1995; Kleinhans et al., 2006) and the importance of lateral flow and sediment fluxes upstream of the bifurcation (Bolla Pittaluga et al., 2003; Kleinhans et al., 2008; Miori et al., 2012; Hardy et al., 2011). This research removed any influence caused by bends in the flow and applied unerodable banks. The results in physical models agree with the BRT model.

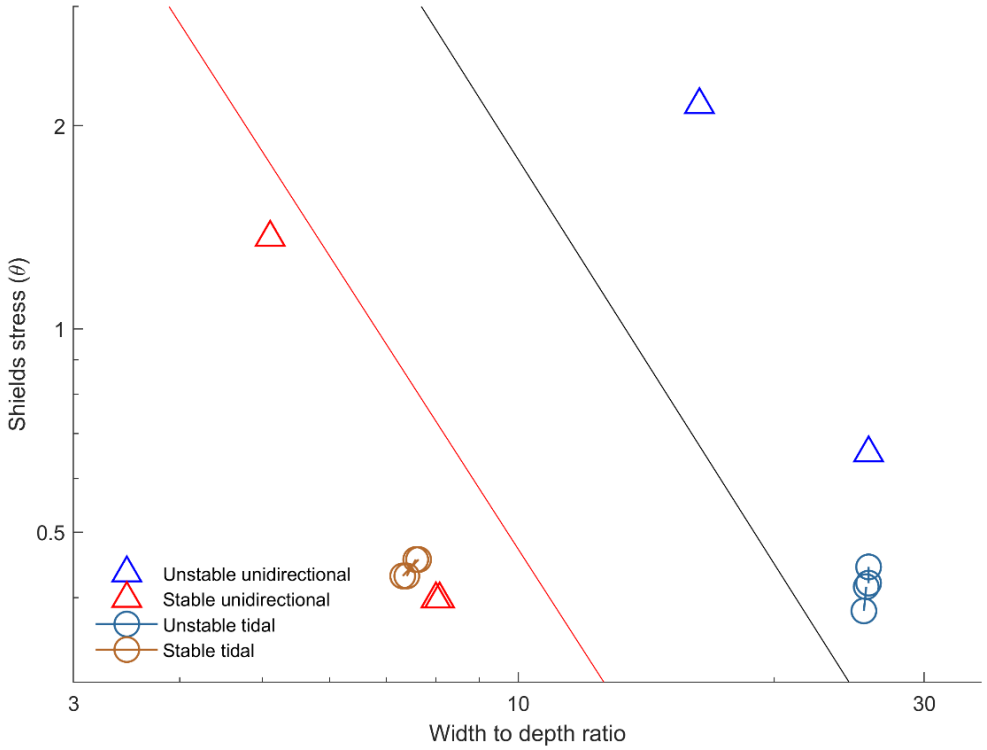

Figure 4.1 Stability diagram plotting Shields stress against width to depth ratio with experimental data plotted as triangles for unidirectional experiments and circles connected by lines for tidal experiments. The circle representing either side up/down stream of the bifurcated channels. Red and orange colours represent stable results while the blue results represent the unstable experiments. The red and black line represent the relationship of α * r being respectively 1 or 2, as given by Bolla Pittaluga et al., 2015.

4.2 Tidal bifurcation

Tidal bifurcations have not yet seen the same amount of research as have the fluvial systems. Research on tidal flows around bifurcations and bars has been done (Buschman et al., 2010; Kastner et al., 2017), and consequently a better understanding of the morphology of tidal bars has been achieved. General understanding and data are still limited on this specific topic. The tidal experiments done in this research provide the first ever experimental data on bifurcation with bidirectional flows. Only symmetrical flow conditions were tested however due to time constraints, but asymmetric tides would be possible in a similar setup. So far it has been impossible to properly model the implications of tidal flow on bifurcation stability because of how hard it is to implement all the different flow computation in combination with good morphological equations. The work by Buschman et al. (2010) shows that there is a very complex system in place where both fluvial and tidal flows collide. They found that the river discharge influenced by tides splits over the two sea-connected channels as a function of differences in their depth, length or bed roughness as they illustrate in figure 4.2. Adding tides to the modelled bifurcations can enhance the inequality in discharge distribution that would already be caused by the fluvial flow. The model results from this research show that depth difference have a large effect and the discharge asymmetry between channels and that tidal motion enhances inequalities in discharge. A big difference with this research compared to the experiments executed for this thesis is that the bifurcate channels would not reconnect

in a confluence. The trends found in the paper by Buschman et al. (2010) suggest an increase in the asymmetry while the results in this thesis would suggest a decrease in asymmetry, and a slower development in the morphology. The reason for this difference could be found in the fact that morphological changes were not considered while it is a big factor in our experiments. Kastner et al. (2017) concluded that certain sediment grainsizes could indeed result in stable asymmetric bifurcation configurations. They did however also conclude that it was of importance to the morphological stability of the channels whether the systems reconnected before reaching the sea.

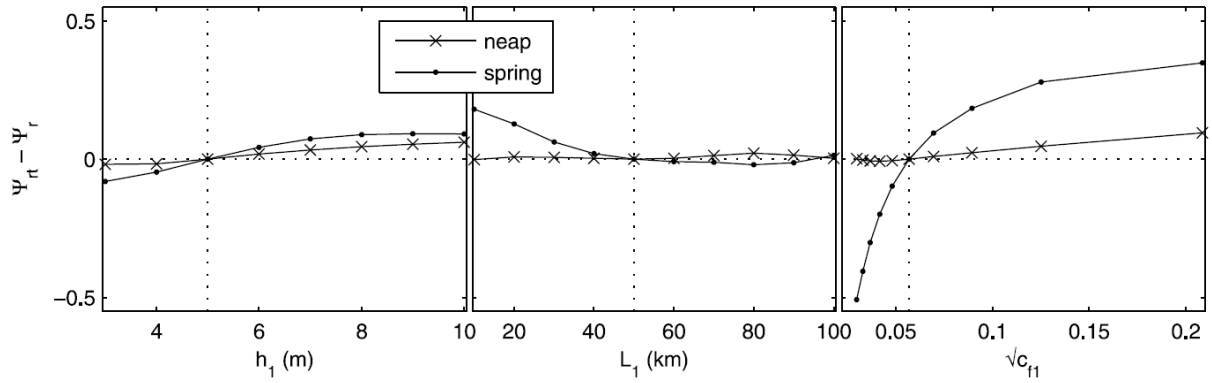

Figure 4.2 The effect of adding tides to a shallow junction system forced with river discharge only on the discharge asymmetry index as a function of (left) depth, (middle) channel length, and (right) the square root of the bed friction coefficient in channel 1. The vertical dashed lines denote the value of the variables in the channel (Buschman et al., 2010).

The length of the used splitter plate was based upon the paper by Leuven et al. (2016) predicting bar length for the width of the system that we investigated. The research done by Leuven does describe tidal bars to be highly unstable and evolving morphological features. Cycles of bar generation and erosion in Leuven at al. (2017 & 2018) show the evolution of bifurcations. Schuurman & Kleinhans (2015) researched behaviour of river bars and the bifurcations they form in braided sand bed rivers showing a lot of similarities to the tidal bars in estuaries. The migration and evolution of the bars, and bifurcation angle that follows from it, forms a major driving force in the bifurcation stability. Our experiments however do not allow for such migration. The first results suggest a similar relationship between width to depth ratio and Shields stress exists as for fluvial bifurcations. Further research into tidal bifurcation stability could help the integration of the functions found in this research into models and improve dynamic forecasting of tidal bars in estuaries.

4.3 Further research

Although the research succeeded in providing experimental data for unidirectional intermediate and high Shields stress conditions, it indicates how little is still known about tidal bifurcations. This research was limited to only two experimental conditions and symmetrical tides. These first results would suggest a similar relation between Shields stress conditions and width to depth ratio of the tidal systems, but the addition of two directions of flow opens a whole new range of parameters that should be tested. As such, future research should consider a similar setup as the one presented here, with bed consisting of both a bifurcation and confluence, but also systems with only a single junction with both channels

ending in a sea. Furthermore, the effect of either symmetrical or asymmetrical tidal conditions should be tested and further investigated. As only a single short perturbation was added to one of the channels in this thesis it should also be investigated what the influence of perturbation in both the channels is (at different locations in the channel). For the tidal experiments, different width to depth ratios for the upstream and downstream channels should also be considered, as these experiment only considered same sized channels. Using the experimental data collected here the models that already exist could be compared and added onto.

Further experiments would have to be conducted in facilities such as the one used in these experiments with an ability to produce flows in both directions. Another facility able of producing the required flows would be the Metronome at the University of Utrecht. A setup within this 20-meter-long and 3-meter-wide flume could be conceived by creating a sea on the two far sides of the flume and dividing the flume in channels with a width of 60 cm. By using splitter plates to bifurcate these channels similar experiments could be conducted as have been conducted in the fast flow facility. This setup would be able to conduct experiments for both symmetrical and asymmetrical tides and have the ability to introduce river discharge. Due to the possibility to run shorter tidal periods and a shorter time required to scan the bathymetry it would be possible to get a more extensive timeseries to check with model results. Using a channel width of only 60 cm will allow for 5 experiments to be ran at the same time, although these would be limited to running the same tidal signal.

5 Conclusions

The aim of this research was to test bifurcation stability forced by upstream channel width to depth ratio and sediment mobility. The experiments were executed for unidirectional flows, for conditions of high sediment mobility and for reversing tidal flow conditions in a symmetrical setup with unerodable banks, an idealized bar and removed all influences of curvature or sediment roughness induced transverse flow.

In accordance with the theory of Bolla Pittaluga et al. (2015), bifurcations with a low width to depth ratio reduced the initial bed level perturbation and discharge inequality, proving that for these configurations bifurcations are stable. Higher width to depth ratios would however result in an increase in channel bed level differences and a larger discharge inequality between the channels increasing the asymmetry introduced by the perturbation. In these experiments, sedimentation upstream of the perturbation would form a transverse slope into the eroding channel while lower width to depth ratios displayed less transverse morphology differences. High sediment mobility experiments at different width to depth ratios were also tested and show the same trends for width to depth ratio. The difference in bed level and discharge inequality between the two channels decreased for high width to depths ratios and increased for lower width to depth ratios. The results confirm that the width to depth ratio of the channel just upstream of the bifurcation is an important parameter for predicting stability, for idealized symmetrically divided channels without curvature and unerodable banks. They also confirm that the same relation applies to high mobility.

Intermediate peak Shields stress conditions for both high and low width to depth ratios were also tested for symmetrical tidal flows. A similar pattern of sedimentation upstream of the perturbation and the evolution of a larger transverse bed slope as seen in the unidirectional experiments is present in the tidal results. This means that the tidal results adhere to a similar stability as the unidirectional experiments although the differences would not evolve as much as in the unidirectional experiments during the same amount of time. With a low width to depth ratio the initial perturbation decreases and the difference in channel bed level was smaller at the end of the experiment. No, or almost no, transverse bed slope would form on either the upstream or downstream side of the bifurcated channels. The experiments done at high width to depth ratios resulted in growth of the perturbation and an increased difference between the two channels bed levels.

This research provides data that were previously unavailable and should prove to be important for a better understanding of bifurcation evolution and stability in both fluvial and tidal channel systems. The produced data align well with tested model results and should thus also prove valuable for testing new and old models' parameters.

6 References

Aslan A, AutinW, Blum M. 2005. Causes of river avulsion: insights from the late Holocene avulsion history of the Mississippi River, USA. *Journal of Sedimentary Research* 75: 650–664.

Baar, A. W., de Smit, J., Uijttewaal, W. S., & Kleinhans, M. G. (2018). Sediment transport of fine sand to fine gravel on transverse bed slopes in rotating annular flume experiments. *Water Resources Research*, *54*(1), 19-45.

Bertoldi, W., & Tubino, M. (2007). River bifurcations: Experimental observations on equilibrium configurations. *Water Resources Research*, *43*(10).

Bertoldi, W., Zanoni, L., Miori, S., Repetto, R., & Tubino, M. (2009). Interaction between migrating bars and bifurcations in gravel bed rivers. *Water resources research*, *45*(6).

Bolla Pittaluga, M., Repetto, R., & Tubino, M. (2003). Channel bifurcation in braided rivers: equilibrium configurations and stability. *Water Resources Research*, *39*(3).

Bolla Pittaluga, M., Coco, G., & Kleinhans, M. G. (2015). A unified framework for stability of channel bifurcations in gravel and sand fluvial systems. *Geophysical Research Letters*, *42*(18), 7521-7536.

Buschman, F. A., Hoitink, A. J. F., Van Der Vegt, M., & Hoekstra, P. (2010). Subtidal flow division at a shallow tidal junction. *Water Resources Research*, *46*(12).

Canestrelli, A., Fagherazzi, S., Defina, A., & Lanzoni, S. (2010). Tidal hydrodynamics and erosional power in the Fly River delta, Papua New Guinea. *Journal of Geophysical Research: Earth Surface*, *115*(F4).

Coco, G., Zhou, Z., Van Maanen, B., Olabarrieta, M., Tinoco, R., & Townend, I. (2013). Morphodynamics of tidal networks: advances and challenges. *Marine Geology*, *346*, 1-16.

Edmonds, D. A., & Slingerland, R. L. (2008). Stability of delta distributary networks and their bifurcations. *Water Resources Research*, *44*(9).

Garde RJ, Ranga Raju KG. 1978. Mechanics of Sediment Transportation and Alluvial Stream Problems. *Wiley: New Delhi*; 483.

Hardy, R. J., Lane, S. N., & Yu, D. (2011). Flow structures at an idealized bifurcation: a numerical experiment. *Earth Surface Processes and Landforms*, *36*(15), 2083-2096.

Ikeda S, Parker G, Sawai K. 1981. Bend theory of river meanders, part 1: linear development. *Journal of Fluid Mechanics* 112: 363–377.

Kästner, K., Hoitink, A. J. F., Vermeulen, B., Geertsema, T. J., & Ningsih, N. S. (2017). Distributary channels in the fluvial to tidal transition zone. *Journal of Geophysical Research: Earth Surface*, *122*(3), 696-710.

Kleinhans, M. G., Cohen, K. M., Hoekstra, J., and IJmker, J. M. (2011). Evolution of a bifurcation in a meandering river with adjustable channel widths, rhine delta apex, the netherlands. *Earth Surface Processes and Landforms,* 36(15).

Kleinhans, M. G., Ferguson, R. I., Lane, S. N., and Hardy, R. J. (2013). Splitting rivers at their seams: bifurcations and avulsion. *Earth Surface Processes and Landforms,* 38(1):47{61.

Kleinhans, M. G., Jagers, H. R. A., Mosselman, E., and Slo_, C. J. (2008). Bifurcation dynamics and avulsion duration in meandering rivers by one-dimensional and three-

dimensional models. *Water resources research,* 44(8).

Kleinhans, M. G., Van Scheltinga, R. T., Van Der Vegt, M., and Markies, H. (2015). Turning the tide: growth and dynamics of a tidal basin and inlet in experiments. *Journal of Geophysical Research: Earth Surface,* 120(1):95{119.

Leopold LB, Wolman MG. 1957. River channel patterns: braided, meandering and straight. *US Geological Survey Professional Pape*r 282-B: 39–85.

Leuven, J. R. F. W., Kleinhans, M. G., Weisscher, S. A. H., & Van der Vegt, M. (2016). Tidal sand bar dimensions and shapes in estuaries. *Earth-science reviews*, *161*, 204-223.

Leuven, J. R. F. W., De Haas, T., Braat, L., & Kleinhans, M. G. (2017). Topographic forcing of tidal sandbar patterns for irregular estuary planforms. *Earth Surface Processes and Landforms*, *43*(1), 172-186.

Leuven, J. R., Braat, L., van Dijk, W. M., de Haas, T., van Onselen, E. P., Ruessink, B. G., & Kleinhans, M. G. (2018). Growing forced bars determine nonideal estuary planform. *Journal of Geophysical Research: Earth Surface*, *123*(11), 2971-2992.

Miori S, Repetto R, Tubino M. 2006a. A one-dimensional model of bifurcations in gravel bed channels with erodible banks. *Water Resources Research* 42: W11413.

Miori S, Repetto R, Tubino M. 2006b. Unsteadiness effects on the morphological behaviour of gravel-bed river bifurcation. In *River Flow 2006*, Ferreira R, Alves E, Leal J, Cardoso A (eds). International Conference on Fluvial Hydraulics, Lisbon, Portugal. Taylor and Francis/Balkema: London UK; 1283–1291.

Miori, S., Bertoldi, W., Repetto, R., Zanoni, L., & Tubino, M. (2007, December). The effect of alternating bars migration on river bifurcation dynamics. In *AGU Fall Meeting Abstracts*.

Miori, S., Hardy, R. J., & Lane, S. N. (2012). Topographic forcing of flow partition and flow structures at river bifurcations. *Earth Surface Processes and Landforms*, *37*(6), 666-679.

Neary VS, Odgaard AJ. 1993. Three-dimensional flow structure at open channel diversions. *Journal of Hydrology England* 119: 1223–1230.

Rice SP, Roy AG, Rhoads B (eds). 2008. River Confluences, Tributaries and the Fluvial Network. *Wiley: Chichester*; 456.

Schuurman, F., & Kleinhans, M. G. (2015). Bar dynamics and bifurcation evolution in a modelled braided sand-bed river. *Earth surface processes and landforms*, *40*(10), 1318-1333.

Seminara, G., Lanzoni, S., & Cecconi, G. (2011). Coastal wetlands at risk: learning from Venice and New Orleans. *Ecohydrology & Hydrobiology*, *11*(3-4), 183-202.

Slingerland R, Smith N. 1998. Necessary conditions for a meandering river avulsion. *Geology 26*: 435–438.

Thomas RE, Parsons DR, Sandbach SD, Keevil GM, Marra WA, Hardy RJ, Best JL, Lane SN, Ross JA. 2012. An experimental study of discharge partitioning and flow structure at symmetrical bifurcations*. Earth Surface Processes and Landforms*. DOI: 10.1002/esp.2231, published online October 2011.

van Veen, J. (1949). Eb-en vloedschaar systemen in de nederlandse getijwateren-ebb and ood channel systems in the netherlands tidal waters. *Technical report, KNAG-TU Delft*.

Wang, Z. B., De Vries, M., Fokkink, R. J., & Langerak, A. (1995). Stability of river bifurcations in ID morphodynamic models. *Journal of Hydraulic Research*, *33*(6), 739-750.

Wang, Z. B., Hoekstra, P., Burchard, H., Ridderinkhof, H., De Swart, H. E., & Stive, M. J. F. (2012). Morphodynamics of the Wadden Sea and its barrier island system. *Ocean & coastal management*, *68*, 39-57.

Wright LD. 1977. Sediment transport and deposition at river mouths: a synthesis. *Geological Society of America Bulletin* 88: 857–868.

Zolezzi G, Bertoldi W, Tubino M. 2006. Morphological analysis and prediction of river bifurcations. In *Braided Rivers: Processes, Deposits, Ecology and Management*, Sambrook Smith GH, Best JL, Bristow CS, Petts GE (eds). International Association of Sediment Special Publication 36: Malden, MA; 233–256.

7 Appendixes

7.1 A

Table A1 Start and stop times and flume settings

Experiment	date	start time	end time	dura-tion (hr)	Pump speed (Hz)	still water level (mm)	water level at flow (mm)	target velocity (m/s)	Pertubation	remarks
1a	5-4-2018	17:25	17:45	00:20	-2	992.8	996.8	0.39	4m (2.5cm) LHS	wave maker not parked
2a	5-4-2018	17:49	18:00	00:11	-3.4	994.2	unknown	0.39	4m (2.5cm) LHS	wave maker not parked
3a	5-4-2018	18:33	19:05	00:32	-4	997.1	1012.3	0.39	4m (2.5cm) LHS	wave maker not parked
4a	5-4-2018	19:11	21:56	02:45	-5	997.1	1022.7	0.39	4m (2.5cm) LHS	water level rose slowly
4b	6-4-2018	09:11	14:16	05:05	-5	992	1016.4	0.39		
4c	9-4-2018	09:55	15:05	05:10	-5	992.4	1015.8	0.39		pressure sensors not recording
5a	11-4-2018	16:00	08:30	16:30	-11	1353.8	1363.5	0.45	4m (2.5cm) LHS	vectrino not recorded after 2.5 hrs pc crash
5b	12-4-2018	11:00	15:42	04:42	-11	1353.7	1364.8	0.45		
5c	12-4-2018	18:23	08:25	14:02	-11	1351.3	1427	0.45		water level rose slowly
6a	17-4-2018	10:29	13:11	02:42	-10.8 /8.6	1347.8	~1390/~1300	0.45	4m (2.5cm) LHS	one pump stopped, terminated after 7 min unidirectional and terminated
6b	17-4-2018	14:12	23:30	09:18	-10.8 /8.7	1347.8	1390/1295	0.45		pumps stopped at about 22:30, switched of 23:30
6c	18-4-2018	10:00	16:00	06:00	-10.8 /8.8	1349.5	1390/1300	0.45		
7a	23-4-2018	10:00	10:20	00:20	-5 /3.4	990	unknown	0.40	4m (2.5cm) RHS	
7b	23-4-2018	14:00	08:08	18:08	-5 /3.4	990	1015/970	0.40		
8a	24-4-2018	11:26	16:01	04:35	-10.8 /8.6	1348.5	1385/1300	0.45	bed after experiment 7	
8b	24-4-2018	16:18	07:18	15:00	-10.8 /8.6	1348.5	1385/1300	0.45		
9a	26-4-2018	11:53	12:00	00:07	-13	1099.7	1155	0.90	4m (4.5cm) RHS	
9b	26-4-2018	12:05	13:08	01:03	-13	1099.7	1151	0.90		

9c	27-4-2018	10:30	11:33	01:03	-13	1098.5	1146	0.90	
10a	30-4-2018	16:00	10:32	18:32	-11	1350	1360	0.90	4m (3.5cm) LHS
11a	1-5-2018	13:45	07:45	18:00	-5/3.4	987.5	unknown	0.40	Bed after experiment 10
11b	2-5-2018	11:45	07:45	20:00	-5/3.4	986.5	1010/968	0.40	
12a	3-5-2018	13:45	14:15	00:30	-5/3.4	1648.8	1660	0.81	Bed after experiment 11
12b	3-5-2018	14:51	15:15	00:24	-5/3.4	1648.8	1660	0.81	

Table A2 Relation between discharge and set pump frequency and water depth.

Pump speed (hz)	water depth (m)	Measured discharge (m^3s^{-1})
-5	0.14	0.22
-10	0.25	0.64
-11	0.5	0.8
-13	0.25	0.77
-14	0.25	0.82
-24	0.5	1.75
-33	0.8	2.4
3.3	0.14	0.21
3.5	0.14	0.23
8	0.25	0.73
9	0.25	0.84
17	0.5	1.76
17.7	0.5	1.82